Germ-free mice exhibit profound gut microbiota-dependent alterations of intestinal endocannabinoidome signaling

Claudia Manca[1,2,7,8], Besma Boubertakh[1,2,8], Nadine Leblanc[1,3,8], Thomas Deschênes[3,4,8], Sebastien Lacroix[1,3,8], Cyril Martin[1,8], Alain Houde[3,8], Alain Veilleux[3,4,8], Nicolas Flamand[1,2,8], Giulio G. Muccioli[5], Frédéric Raymond[3,4,8], Patrice D. Cani[6], Vincenzo Di Marzo[1,2,3,4,7,8], Cristoforo Silvestri[1,2,8,*]

1 Centre de recherche de l'Institut universitaire de cardiologie et de pneumologie de Québec (IUCPQ), Québec, Canada;

2 Département de médecine, Faculté de Médecine, Université Laval, Québec, Canada

3 Institut sur la nutrition et les aliments fonctionnels (INAF), Québec, Canada;

4 École de nutrition, Faculté des sciences de l'agriculture et de l'alimentation (FSAA), Université Laval, Québec, Canada

5 Université Catholique de Louvain, UCLouvain, Louvain Drug Research Institute (LDRI), Bioanalysis and Pharmacology of Bioactive Lipids Research Group (BPBL), Brussels, Belgium

6 Université Catholique de Louvain, UCLouvain, Louvain Drug Research Institute, Walloon Excellence in Life Sciences and Biotechnology (WELBIO), Metabolism and Nutrition Research Group, Brussels, Belgium

7 Joint International Unit between the National Research Council (CNR) of Italy and Université Laval on Chemical and Biomolecular Research on the Microbiome and its Impact on Metabolic Health and Nutrition (UMI-MicroMeNu), Institute of Biomolecular Chemistry, CNR, Pozzuoli, Italy.

8 Canada Excellence Research Chair in the Microbiome-Endocannabinoidome Axis in Metabolic Health (CERC-MEND)

*to whom correspondence should be addressed

cristoforo.silvestri@criucpq.ulaval.ca

Running title: The endocannabinoidome without a microbiome

Abbreviations: all the abbreviations are listed in Supplementary Table S1 and S4.

JOURNAL OF LIPID RESEARCH ASBMB

Abstract

The gut microbiota is a unique ecosystem of microorganisms interacting with the host through several biochemical mechanisms. The endocannabinoidome (eCBome) - a complex signaling system including the endocannabinoid system, approximately 50 receptors and metabolic enzymes, and more than 20 lipid mediators with important physiopathologic functions modulates gastrointestinal tract function and may mediate host cell-microbe communications there. Germ-free (GF) mice, which lack an intestinal microbiome and so differ drastically from conventionally reared (CR) mice, offer a unique opportunity to explore the eCBome in a microbe-free model and in the presence of a reintroduced functional gut microbiome through fecal microbiome transfer (FMT). We aimed to gain direct evidence for a link between the microbiome and eCBome systems by investigating eCBome alterations in the gut in GF mice before and after FMT. Basal eCBome gene expression and lipid profiles were measured in various segments of the intestine of GF and CR mice at juvenile and adult ages using targeted qPCR transcriptomics and LC-MS/MS lipidomics. GF mice exhibited age-dependent modifications in intestinal eCBome gene expression and lipid mediator levels. FMT from CR donor mice to age-matched GF male mice reversed several of these alterations, particularly in the ileum and jejunum, after only 1 week, demonstrating that the gut microbiome directly impacts the host eCBome and providing a cause-effect relationship between the presence or absence of intestinal microbes and eCBome signaling. These results open the way to new studies investigating the mechanisms through which intestinal microorganisms exploit eCBome signaling to exert some of their physiopathologic functions.

Key words

endocannabinoidome, endocannabinoids, gut microbiome, germ free phenotype, intestine, fecal microbiota transfer, gene expression, lipidomics.

Introduction

The gut microbiome represents an array of different microorganisms that unevenly colonize the surfaces of the gastrointestinal tract. Considering its active biomass and metabolic function, it can be considered as a true organ in the body (1), exerting a profound impact on adult and early human health and playing a potential role in specific diseases (2). Intestinal bacteria have specific functions in host nutrient, xenobiotic and drug metabolism, the maintenance of structural integrity and immune-competence of the gut mucosal barrier (3). They influence several other organ systems, including the central nervous system, adipose tissue and the liver (4–6). Individual populations of microbiota exist within characteristically distinct regions along the length of the gastrointestinal tract, with the colon having the greatest proportion (7, 8). These individual populations can be affected by host and host-related characteristics, such as gender, age, genetics, as well as the diet and other environmental factors (9–11).

Germ Free (GF) mice provide a useful experimental tool to understand microbiota-host interactions and dissect their molecular mechanism. These mice have a characteristic phenotype, showing several developmental and physiological differences with respect to conventionally raised (CR) mice (12). At the gastrointestinal level, they display alterations in gut morphology, motility, absorption, secretion and immune function. The cecum of GF mice is enlarged by 4-8-fold because of mucus and undigested fiber accumulation, and the small intestine is less developed (12), with reduced epithelial cell turnover and irregular microvilli (13) along with decreased gut motility partly due to decreased innervation with sensory neurons (14). Despite the absence of microbially produced short chain fatty acids (SCFAs), GF mice were also demonstrated to have increased levels of colon-derived and circulating glucagon-like peptide-1 (GLP-1) that did not improve the incretin response but instead slowed small intestinal transit potentially as an adaptive response, promoting nutrient absorption in the face of insufficient energy availability (15). GF mice also exhibit decreased or absent expression of several Toll like receptors, essential for the recognition of pathogen-associated molecular patterns (16), poorly formed Peyer's patches, and alterations of the composition of CD4+ T cells and IgA-producing B cells in the lamina propria, with impaired development and maturation of isolated lymphoid follicles (17).

Some perturbations of the gut microbiota, generally defined as "dysbiosis", may cause a decrease of intestinal barrier integrity, and the subsequent entry into the bloodstream of bacterial constituents such as

lipopolysaccharides (LPS) from gram-negative bacteria, which trigger the onset of low-grade inflammation contributing to, among others, insulin resistance (18). It has been suggested that this pathological condition occurs via the over-activation of the cannabinoid receptor type-1 (CB1) (19), thus highlighting the potential relationship between microbiota dysbiosis and the endocannabinoid (eCB) system. This is a pleiotropic signaling system composed of CB1 and cannabinoid type-2 (CB2) receptors, their two lipid ligands, the endocannabinoids (eCBs) *N*-arachidonoylethanolamine (anandamide, AEA) and 2-arachidonoyl-glycerol (2-AG), and eCB anabolic and catabolic enzymes. These enzymes, include, among others, *N*-acylphosphatidylethanolamine-hydrolysing phospholipase D (NAPE-PLD) and fatty acid amide hydrolase (FAAH), respectively, for AEA, and diacylglycerol lipases (DAGL) α and β and monoacylglycerol lipase (MAGL), respectively, for 2-AG (20). It is well established that AEA and 2-AG are often accompanied in tissues by their congeners, the *N*-acylethanolamines (NAE) and 2-acylglycerols, as well as by other amides of long chain fatty acids with amino acids or neurotransmitters (21). Both eCB congeners, which share with the eCBs the same anabolic and catabolic enzymes, and other eCB-related amides, which occasionally can be inactivated by FAAH, interact with receptors other than CB1 and CB2, including some transient receptor potential (TRP) channels, peroxisome proliferator-activated receptors (PPARs), and some orphan G protein-coupled receptors, which are also activated by other non-eCBome ligands. Oxidation of AEA and 2-AG and some of their arachidonic acid (AA)-containing congeners by AA-metabolizing enzymes also leads to yet another series of emerging bioactive lipids (21). This wide range of lipid mediators, receptors and enzymes, including and extending the eCB system, has been defined as the "endocannabinoidome" (eCBome) (22, 23).

The eCBome modulates several physiological functions, including gastrointestinal tract function, energy homeostasis and metabolism (24). Tissue and circulating levels of eCBome molecules are altered by dietary factors (and particularly, in view of their chemical nature, by the fatty acid composition of the diet) as well as by gut microbiota. For example, a high fat diet alters gut microbiota, which control intestinal eCBome tone by altering NAPE-PLD, CB1 and FAAH expression, and AEA levels resulting in increased intestinal permeability and decreased adipogenesis in obese mice (19). A recent study showed that chronic treatment with antibiotics, leading to dysbiosis without erasing the gut microbiota population, can alter the levels of NAEs and *N*-acyl-serotonins in the small intestine (25). On the other hand, NAPE-PLD deletion in white adipocytes or intestinal epithelial cells induces dysbiosis and related dysmetabolism, possibly also due to the reduction of the local

tissue concentrations of some NAEs and subsequently impaired signaling of non-cannabinoid receptors (26, 27).

So far, however, no study has been conducted to define how the eCBome is altered in the increasingly used GF mouse model, which lacks an intestinal microbiome and offers the unique possibility, through fecal microbiome transfer, to look at the effects on animal physiological pathways of reintroducing, in part or completely, a functional gut microbiome. In the present study, we therefore assessed the basal eCBome gene profiles within GF and conventionally raised male mice at juvenile and adult ages and we correlated these results with eCBome lipid mediator levels. We also assessed the effect of a fecal microbiota transfer (FMT) on the potentially altered eCBome. We focused on the small and large intestine where the largest microbial populations reside in mammals, and the most profound alterations due to its absence are likely to occur.

Materials and Methods

Animals and housing

Conventionally Raised (CR) and Germ free (GF) C57BL/6NTac mice were purchased from Taconic (Taconic Bioscience, NY, USA) and maintained in the animal facility of the Institut Universitaire de Cardiologie et Pneumologie de Québec (IUCPQ, QC, Canada). All animals were grouped 3-4 mice per cage under a 12h:12h light dark cycle with *ad libitum* access to NIH-31 Open Formula Autoclavable Diet (Zeigler, PA, USA) and water. GF mice were housed in axenic status and fecal samples were weekly tested for microbes and parasites by the facility's staff to ensure that the GF unit was indeed sterile. Both GF and CR mice were acclimatized for at least one week prior to start with the procedures.

In order to confirm gene expression data, we also used mice housed within a different animal facility. C57BL/6J 8-weeks old male mice were purchased from Charles River laboratories (France) and were housed in a specific and opportunistic pathogen free (SOPF) animal facility with a controlled temperature-humidity and 12h light-dark cycle (6am light/6pm dark). Mice had with free access to water and food (A04, Villemoisson sur Orge, France). Swiss-Webster conventional mice or germ-free male mice (7-week-old) from Taconic were also used in the transplantation study.

Animal experiments and Fecal Microbial Transplant (FMT)

6 male CR and GF mice at 4 and 13wk of age were intraperitoneally anesthetized with a cocktail of ketamine/xylazine/acepromazine at a dose of 50/10/1,7 mg/kg body weight and euthanized by intra-cardiac puncture. Whole blood was collected in K3-EDTA tubes. The abdominal cavity was opened and the whole digestive tract was carefully aligned from the stomach up to the colon. Once the stomach was removed, the small (duodenum, jejunum, ileum) and large (cecum and colon) intestine were carefully excised and separated and the intestinal contents were harvested by flushing with 1ml of sterile PBS without Ca/Mg (Thermo Fisher Scientific, MA, USA) and snap frozen. Sections of small and large intestine were both stored either in RNALater (Thermo Fisher Scientific, MA, USA) for RNA stabilization or immediately snap frozen and stored at -80°C for further analysis. This common procedure was concluded, for each mouse, within a maximum of 15 minutes, a time frame that allowed for the preservation of mRNA and lipid for the further analysis. All the

experimental protocols were validated by the approved by Laval University animal ethics committee (CPAUL 2018010-1).

For fecal microbiota transplant (FMT) experiments, GF mice were randomly divided into two groups at the age of 12wk; those gavaged with sterile PBS (SHAM; 5 mice) and those gavaged with fecal material (FMT; 6 mice). Material gavaged for FMT consisted of the intestinal contents and stools of a single and 4 CR donor mice respectively. Briefly, duodenum, jejunum, ileum, colon and cecum intestinal contents were collected from one 12wk old CR donor mouse and were mixed with stool pellets all the CR mice to be used as controls. The mixture was well homogenized, weighed, suspended 1:10 in sterile PBS and centrifugated at 805xg for 10 minutes at RT. The supernatant was used to gavage the mice (200µl of homogenate/mouse). The FMT mice were then housed (3 per cage) for one week in conventional conditions in cages contaminated with used litter coming from donor mice cages. CR mice were euthanized the day of the gavages while SHAM and FMT mice were sacrificed one week after the gavage; plasma, tissues and intestinal contents were collected from all the animals as previously described (for an outline of the experimental protocol see Fig.1).

The mice utilized for Fig. 2E and F were anesthetized using intraperitoneal (i.p.) ketamine and xylazine at concentrations of 100 and 10 mg/kg, respectively, after a 5-h fasting period. Tissues were harvested for further analysis. Mice were killed by cervical dislocation. The intestinal segments (jejunum, ileum and colon) were precisely dissected and immersed in liquid nitrogen and stored at -80°C for further analysis.

Swiss-Webster GF mice were conventionalized with the gut microbes (i.e., cecal content) from male conventional Swiss-Webster mice and maintained in individualized ventilated cages (IVC AERO GM500, Tecnilab-BMI).

Antibiotic treatment

C57BL/6J mice were treated with ampicillin (1 g/l; Sigma) and neomycin (0.5 g/l; Sigma) in their drinking water for 2 weeks (19).

RNA isolation, Reverse Transcription and qPCR-based TaqMan Open Array

RNA was extracted from the duodenum, jejunum, ileum and colon samples with the RNeasy Plus Mini Kit (Qiagen, Hilden, Germany) following the manufacturer's instruction and eluted in 50µl of UltraPure Distilled Water (Invitrogen, CA, USA). The concentration and purity of RNA was determined by measuring the

absorbance of the RNA in a Biodrop at 260nm and 280nm, and RNA integrity was assessed by an Agilent 2100 Bioanalyzer, using the Agilent RNA 6000 Nano Kit (Agilent Technologies, CA, USA). 1µg of total RNA was reverse transcribed using the iScript cDNA synthesis kit (Bio-Rad, CA, USA) in a reaction volume of 20µl. 60ng of starting RNA was used to evaluate the expression of the 52 eCBome-related genes and 4 housekeeping genes (Suppl. Table 1) using a custom-designed qPCR-based TaqMan Open Array on a QuantStudio 12K Flex Real-Time PCR System (Thermo Fisher Scientific, CA, USA) following the manufacturer's instruction. The mRNA expression levels of 14 eCBome genes were validated using the same cDNA and specific forward and reverse primer pairs (IDT, IA, USA) (Suppl. Table 2) on a CFX384 touch qPCR System (BioRad) using PowerUp SYBR Green qPCR master mix (Thermo Fisher Scientific, CA, USA) in duplicate reactions. *Hprt1* and *Tbp* were used as reference genes for all qPCR assays. Based on the fact that the Ct of the reference genes were the same in all the 13wk old control samples (first and FMT experiments), we merged the two control sets into one 13wk control group. Gene expression levels were evaluated by the $2^{-\Delta\Delta Ct}$ method and represented as fold increase with respect to baseline within each tissue section for each age. Target genes were, however, differentially expressed in the different intestinal segments, as shown by differences in Ct, summarized in Suppl. Table 3.

The intestinal gene expression levels of *Gpr55* was also assessed in another institute as follow: total RNA was prepared from tissues using TriPure reagent (Roche), cDNA was synthesized from 1mg of total RNA using a reverse transcription kit (Promega Corp.) and qPCR were performed by using a STEP one PLUS instrument and software (Applied Biosystems) according to the manufacturer's instructions. RPL19 RNA was chosen as the housekeeping gene and data were analyzed according to the $2^{-\Delta\Delta CT}$ method. The identity and purity of the amplified product were assessed by melting curve analysis at the end of amplification.

Lipid extraction and HPLC-MS/MS for the analysis of eCBome mediators

Lipids were extracted from tissue samples according to the Bligh and Dyer method (28). Briefly, about 10mg of each tissue were homogenized in 1ml of Tris-HCl 50mM pH 7 and methanol (1/1) using a tissue homogenizer; 200µl of the mixture were added to 800µl (1:5 dilution) of the same Tris-HCl/methanol solution containing 0.1M acetic acid and 5ng of deuterated standards. 1ml of chloroform was then added to each sample, vortexed for 30 seconds and centrifuged at 3000×g for 5 minutes. This was repeated twice for a total addition

of 3ml of chloroform. The organic phases were collected and evaporated under a stream of nitrogen and then suspended in 50µl of mobile phase containing 50% of solvent A (water + 1mM ammonium acetate + 0,05% acetic acid) and 50% of solvent B (acetonitrile/water 95/5 + 1mM ammonium acetate + 0.05% acetic acid). 40µl of each sample was finally injected onto an HPLC column (Kinetex C8, 150 × 2.1mm, 2.6µm, Phenomenex) and eluted at a flow rate of 400µl/min using a discontinuous gradient of solvent A and solvent B (27). Quantification of eCBome-related mediators (Suppl. Table 4), was carried out by HPLC system interfaced with the electrospray source of a Shimadzu 8050 triple quadrupole mass spectrometer and using multiple reaction monitoring in positive ion mode for the compounds and their deuterated homologs.

The 13wk old control results were assembled into a single control group. In the case of unsaturared monoacyl-glycerols, the data are presented as 2-monoaclyl-glycercols but represent the combined signals from the 2- and 1(3)-isomers since the latter are most likely generated from the former via acyl migration from the 2- to the *sn*-1 or *sn*-3 position.

DNA extraction and 16S rRNA gene sequencing

DNA was extracted from intestinal contents using the QIAmp PowerFecal DNA kit (Qiagen, Hilden, Germany) according to the manufacturers' instructions. The DNA concentrations of the extracts were measured fluorometrically with the Quant-iT PicoGreen dsDNA Kit (Thermo Fisher Scientific, MA, USA) and the DNAs were stored at −20°C until 16S rDNA library preparation. Briefly, 1ng of DNA was used as template and the V3-V4 region of the 16S rRNA gene was amplified by polymerase chain reaction (PCR) using the QIAseq 16S Region Panel protocol in conjunction with the QIAseq 16S/ITS 384-Index I (Sets A, B, C, D) kit (Qiagen, Hilden, Germany). The 16S metagenomic libraries were eluted in 30µl of nuclease-free water and 1µl was qualified with a Bioanalyser DNA 1000 Chip (Agilent, CA, USA) to verify the amplicon size (expected size ~600 bp) and quantified with a Qubit (Thermo Fisher Scientific, MA, USA). Libraries were then normalized and pooled to 2nM, denatured and diluted to a final concentration of 6pM and supplemented with 5% PhiX control (Illumina, CA, USA). Sequencing (2 × 300 bp paired-end) was performed using the MiSeq Reagent Kit V3 (600 cycles) on an Illumina MiSeq System. Sequencing reads were generated in less than 65 h. Image analysis and base calling were carried out directly on the MiSeq. Data was processed using the DADA2 pipeline (30) and microbiota composition assessed by calculating alpha and beta-diversity indexes

and intra and inter-individual variations in microbial composition using PERMANOVA (vegan R package) (31). Reads were rarefied to 8000 reads to account for depth bias for total FMT pool, colon CR, colon FMT, cecum CR and cecum FMT. Total read counts were used for ileum CR (8088), ileum FMT (4072), jejunum CR (5164) and jejunum FMT (716). Statistical analysis was only performed on colon and cecum as read counts for ileum and jejunum were not sufficiently high to carry out this analysis.

Statistical analysis

Data are expressed as the mean±standard error (S.E.M), as specified in the individual Tables and Figures.

For gene expression analysis, the differences between the CR and GF of 4wk and 13wk old were assessed separately and each intestinal tract was analyzed independently. Particularly, the differences between the CR and GF of 4wk old male mice and the differences between CR and Ab mice were assessed using an unpaired Mann-Whitney T-test on ddCt, while for the 13wk old mice and Swiss Webster mice, One-Way ANOVA followed by Fisher's Least Significant Difference (LSD) test was used. With regard to eCBome mediator levels (pmol/mg), superscript letters represent the differences, in each intestinal tract, between CR and GF 4wk old mice as determined by an unpaired Mann-Whitney T-test and between CR, GF, SHAM and FMT 13wk old mice as determined by a One-Way ANOVA followed by Fisher's Least Significant Difference (LSD) test. The changes of the CR mediators levels between the different intestinal segments at both 4wk and 13wk were also assessed using unpaired Mann-Whitney T-test. For both the 4 and 13wk old analysis, CR and Ab mice and Swiss Webster mice experiments, the differences between experimental groups were considered statistically significant for $p \leq 0.05$ and groups with different superscript letters indicates significant differences. Data were analyzed using Software GraphPad Prism 6.01 (La Jolla, CA, USA).

Principal component analysis was performed using the FactoMineR R package (29).

Results

GF mice exhibit important changes in eCBome signaling that are partially reversed by FMT

To investigate how the absence of the gut microbiota can affect the eCBome, we measured eCBome gene expression and mediator levels within juvenile (4wk) and adult (13wk) GF and CR male mice in the duodenum, jejunum, ileum and the proximal colon. Then, to assess the potential for gut microbiota to subsequently reverse the observed changes in the eCBome, we conventionalized the mice through FMT in 12wk old GF mice and reassessed the eCBome after one week. Although qPCR analyses from different ages and intestinal segments cannot be quantitatively compared as they were run in separate experiments, a comparison of the threshold cycles (Cts) for each gene (see Suppl. Table 3) indicated that the mRNA expression of none of the genes investigated was strongly altered when passing from 4 to 13wk of age.

Whilst several alterations were found in GF mice, we shall discuss hereafter only those that were reversed at some level by the FMT, suggesting that the observed changes in GF mice are directly due to a lack of microbiota and not developmental consequences resulting from their absence or adaptive mechanisms.

Genes encoding eCBome receptors

We observed changes in the expression of *Cnr1*, *Gpr18*, *Gpr55* and *Ppara* within the intestines of GF mice. In general these changes showed similar trends in young and adult GF mice with respect to CR controls in the duodenum, jejunum, ileum and colon, and in some instances, such as for *Gpr18* and *Gpr55* in the ileum, the differences in gene expression became markedly more pronounced with age (Fig. 2B, C).

With regard to *Cnr1* (encoding CB1), while there were no changes in expression at 4wk in any intestinal section, there was a trend to increased expression in the colon, which became statistically significant by 13wk (Fig. 2A). Similarly, ileal *Cnr1* expression increased by ~2-fold in 13wk GF mice. Notably, even though not statistically significant, the FMT partially reversed this change (Fig. 2A). In contrast, the FMT did reverse increased *Cnr1* expression within the colon; however, puzzlingly, the SHAM controls showed the exact same effect, despite having been confirmed to be GF at the point of tissue harvesting.

As for the two orphan G-protein-coupled receptors, *Gpr18* and *Gpr55* (Fig. 2B and 2C), their expression in GF mice was decreased in all tracts of the small intestine at 4wk and 13wk, except in the duodenum for *Gpr55* at 4wk and *Gpr18* at 13wk. As with *Cnr1* in the colon, FMT reversed the observed decreases for both targets

in the jejunum, but SHAMs showed similar effects. However, in the ileum, FMT partially, but significantly rescued the expression of both genes, while no effects were observed in SHAMs. Conversely, *Gpr55* expression in the duodenum was fully and specifically rescued only by FMT (Fig. 2B and C).

In order to confirm the effects observed for *Gpr55* in the ileum, and in view of the increasing importance of the protein encoded by this gene as a receptor for both endocannabinoids and plant cannabinoids, particularly in immune and inflammatory response, we assayed its expression in 7wk old GF Swiss Webster mice housed within a different animal facility. Consistent with results obtained in C57BL/6NTac, *Gpr55* expression was significantly reduced in the ileum of these mice, and conventionalization resulted in a significant reversion of this decrease (Fig. 2E). The regulation of *Gpr55* expression by gut microbes in the ileum was further confirmed through the use of antibiotics, which significantly decreased *Gpr55* expression (Fig. 2F). In GF Swiss Webster mice, or in CR C57BL/6J mice treated with antibiotics, *Gpr55* expression was reduced also in the colon, where again this effect showed a strong tendency toward reversion by conventionalization (Fig. 2E). This supports the identification of a trend observed in the colon of 4 week old C57BL/6NTac mice (Fig. 2C), and suggests a potential age-dependent effect of the lack of gut microbiota on this gene. Finally, the jejunum, Swiss Webster and C57BL/6J mice also showed a trend towards reduction of *Gpr55* expression following GF raising or treatment with antibiotics respectively (Fig. 2E, F), in partial agreement with the results obtained in both 4 week and 13wk old C57BL/6NTac mice.

Pparα expression was increased in all the tracts of the small intestine of GF mice at 4wk, but remained increased only in the duodenum and ileum at 13wk (Fig. 2D). These latter decreases were totally and specifically reversed by the FMT (Fig. 2D).

eCBome mediators

The tone of a given receptor can be altered either by its expression levels and coupling to downstream signaling, by changes in the concentration of its ligand, or both. We therefore next measured a panel of eCBome ligands (Suppl. Table 4) in all tracts of the small intestine and colon to determine if they were altered in 13wk GF mice and if their levels could subsequently be affected by FMT. Not all mediator levels were within the detection limits of the method. Moreover, we present data only for those mediators that, apart from being detectable and quantifiable, underwent alterations in GF, SHAM or FMT mice.

First, we checked if the tissue levels of the mediators varied between 4wk and 13wk old CR mice, and found that in most of the cases when the differences were statistically significant, the concentrations were higher at 4wk, as in the case of AEA and EPEA in the jejunum (P=0.011 and 0.016, respectively) and ileum (P=0.04 and 0.02, respectively), 2-AG in the ileum (P=0.001), DHEA in jejunum, ileum and colon (P=0.022, 0.016 and 0.024, respectively), and LEA, 2-EPG and 2-2DHG in the ileum (P=0.007, 0.02 and 0.004, respectively). The only mediator found to decrease was 2-OG, which was significantly higher at 13wk, although only in the colon (P=0.022). We also observed several statistically significant differences between the levels of the mediators in different intestinal segments at both 4 and 13wk (Suppl. Table 5A and B). In general, 2-acylglycerols were more abundant in proximal intestinal regions than distal ones (the most frequent exception to this rule being 2-OG and 2-LG). By contrast, NAEs tended to show an opposite trend especially at 4wk along the small intestine, with AEA, LEA and DHEA being highest in the ileum.

Next, we analyzed differences due to the GF condition. AEA levels did not show any significant alterations in young GF mice, however they were significantly increased in the jejunum and colon of GF mice at 13wk. While in the jejunum there was no FMT-reversible change observed, the colon displayed a statistical reversion by FMT, though the SHAM showed similar results (Fig. 3A). 2-AG levels on the other hand were only transiently increased in in the jejunum at 4wk, returning to CR levels at 13wk, and not significantly increased in the ileum at 13 wk. Interestingly however, FMT resulted in a significant decrease in jejunal 2-AG levels from those observed in GF mice, and were even lower than those in CR mice. This suggests that the production, or metabolism, of 2-AG within the jejunum, despite no longer being significantly increased in 13wk CR mice, becomes more sensitive to the introduction of bacteria. These results for 2-AG are partly consistent with alterations in the expression of the 2-AG catabolic enzymes MAGL (Suppl. Table 6) and PPT1 at 4wk, and for PPT1 at 13wk (see below, Fig. 5D and Suppl. Table 6).

With regard to *N*-acylethanolamines (Fig. 3A), the most robust changes were observed for *N*-oleoyl-ethanolamide (OEA), *N*-linoleoyl-ethanolamide (LEA), *N*-eicosapentaenoyl-ethanolamide (EPEA) and *N*-docosahexaenoyl-ethanolamide (DHEA). Indeed, the significant increases of OEA, LEA and EPEA in the duodenum of GF adult mice were fully reversed by FMT but not SHAM treatments, while for DHEA, the SHAM also significantly reversed the observed increase in GF mice, though FMT resulted in a stronger effect to levels below that observed in CR mice. The jejunum showed the same trend for OEA, LEA and EPEA,

though the increase was only significant for the latter, and in all cases FMT only resulted in statistically insignificant trends towards decreased levels. In the colon, both OEA and LEA were significantly increased in 4wk GF mice, though this was only maintained in the case of LEA at 13wk, and while FMT completely reversed this effect, so did the SHAM. This same pattern in 13wk mice was observed for EPEA at 13wk.

Regarding monoacylglycerols, while there were no significant changes in 2-OG and 2-LG along the entire intestine at both ages, 2-EPG and 2-DHG levels were significantly increased in the jejunum of 4wk old GF mice (Fig. 3B). The same trend was present in the adult mice, and, as with 2-AG, FMT reduced their levels from those observed in GF mice and, in the case of 2-DHG, to levels lower than those observed in CR mice. However, once again, SHAMs showed similar effects. In the ileum, 2-EPG levels were not significantly increased at 13wk in GF and SHAM mice, and decreased by FMT.

AA, a lipid mediator itself and the ultimate precursor (and metabolite) for both AEA and 2-AG, was significantly increased in the jejunum of young GF mice and a same trend was present in adult mice (Fig 4A), while in the other parts of the small intestine only non-significant trends were observed. However, interestingly, in the ileum, FMT significantly increased AA to levels higher than observed in 13wk CR mice. This however, did not correlate with alterations in AEA or 2-AG levels (Fig. 3A and B). In the colon, AA levels were also significantly increased in GF mice, and reduced by FMT, although the SHAM treatment also produced a similar reduction.

Genes encoding eCBome metabolic enzymes

As for the eCBome anabolic enzymes for AEA and other NAEs, the most significant results were observed for *Abhd4*, *Gde1*, and *Ptpn22*. *Abhdd4* and *Gde1* encode enzymes that in combination provide a NAPE-PLD-independent pathway for NAE synthesis. Both genes were significantly increased in the ileum of 4wk GF mice, which was maintained only in the ileum at 13wk, and completely reversed to levels below those of CR mice specifically by FMT (Fig 5A). *Gde1* expression was similarly affected in the duodenum at 13wk although less markedly. Here too FMT reduced gene expression levels to those below CR mice, while SHAMs had a non-significant decrease (Fig. 5A). Most interestingly, the protein tyrosine phosphatase *Ptpn22*, encoding a multi-function phosphatase suggested to be involved in AEA biosynthesis (32), had the mirror opposite expression in response to GF status to those described above. *Ptpn22* expression was in fact decreased in all sections of

the small intestine at 4wk in GF mice, an effect that was only maintained in the ileum at 13wk. Here again the FMT was specifically able to reverse this effect, but not completely, as with *Abhd4*, *Gde1* (Fig. 5A). These data suggest that two alternate pathways for NAE biosynthesis respond differently to the GF status and subsequent conventionalization.

Concerning the expression levels of eCBome catabolic enzymes for AEA and other NAEs, the expression levels of *Faah* and *Naaa* responded almost identically to the GF status and FMT, and although results were not always statistically significant, trends were maintained (Fig. 5B). The expression of both genes was increased in the duodenums of 13wk GF mice, which was completely reversed by FMT, while SHAMs only showed non-significant decreases. *Faah* and *Naaa* expression also increased in jejunums and ileums of 4 and 13wk GF mice, though this effect was only maintained in a statistically significant manner for *Faah* in the ileums of older mice. Within the jejunums, FMT decreased the expression of both *Faah* and *Naah* from those observed in SHAMs, but not to levels below those observed in GF mice. However, for *Faah*, in the ileum, the increase was completely reversed to CR levels by FMT.

Regarding the gene encoding the enzyme peptidylglycine alpha-amidating monooxygenase (*Pam*), responsible for the biosynthesis of primary fatty acid amides from the oxidative catabolism of the corresponding *N*-acyl-glycines, its expression was increased in all regions of the small intestine of 4wk GF mice. At 13wk *Pam* expression behaved exactly like *Faah* and *Naaa* in the jejunum and ileum of GF mice. Furthermore, in both tissues, FMT always induced a significant reversion to levels observed in CR mice while SHAMs showed no effect (Fig. 5B).

As for the metabolic enzymes for 2-AG and other 2-acyl-glycerols, the most relevant results were found for *Dagla* and *Daglb*, encoding for enzymes that biosynthesize these compounds by catalyzing the hydrolysis of the corresponding diacylglycerols (33, 34), and for the serine hydrolases *Abhd6* and *Ppt1*, which encode for enzymes that have been described to play a role in 2-acyl-glycerol inactivation under certain conditions (35–37) (Fig. 5C and D). In 4wk GF mice, *Dagla* displayed a significant decrease in the jejunum and ileum and, only in the latter did FMT reverse the trend towards decreased expression at 13wk. *Daglb* expression was similarly affected in the jejunum and ileum at both ages, though here the decrease and complete reversion by FMT in ileums was statistically significant and specific (i.e. not observed with SHAMs) (Fig. 5C). The expression levels of *Daglb* were also decreased in the colon of 13wk GF and then totally reverted by the FMT,

while SHAM treatment produced no changes (Fig. 5C). For *Abhd6* and *Ppt1* only the latter showed changes of gene expression in the small intestine at 4wk, where it is consistently downregulated in all regions (Fig. 5D). Interestingly, at 13wk, *Abhd6* and *Ppt1* often show mirror opposite changes in gene expression within individual sections of the small intestine; *Abhd6* is increased, while *Ppt1* is decreased in all regions. FMT results in specific and full rescue of these alterations in all cases, and indeed in the duodenum and jejunum it increases *Ppt1* expression to levels significantly higher than those observed in CR mice at 13wk.

Among the other genes encoding for lipid mediator metabolic enzymes, surprising results came from the analysis of *Pla2g5* (Fig. 4B). This gene encodes a calcium-dependent phospholipase A_2 involved in AA mobilization (and eicosanoid biosynthesis), and phospholipid remodeling and subsequent formation of AEA biosynthetic precursors. The expression of this gene was drastically reduced in a manner significantly and specifically reversed by FMT in all the tracts of the small intestine and colon, with the only exception in the duodenum of 4wk GF mice. Even though the results were not always statistically significant, *Ptges*, encoding the biosynthesizing enzyme for prostaglandins and prostamide E_2, a bioactive metabolite of AEA, also showed a significant reduction (although less marked) in the jejunum and ileum in both 4 and 13wk GF mice, with a similar trend observed in the duodenum. These decreases were totally reversed by FMT but not in SHAMs (Fig. 4C).

Global changes in eCBome gene expression in response to GF status

We found that GF mice are characterized by significant changes in gene expression of several eCBome receptors and metabolic enzymes, both at 4 and 13 weeks of age and in the various parts of the gastrointestinal tract. Most importantly, the successful colonization by gut microbiota partially reversed the changes in expression of several eCBome genes in GF mice, particularly in the various tracts of the small intestine. Accordingly, PCA analysis of the qPCR array data for all genes showed that, for all small intestine segments, CR and FMT mice clustered closely, while GF and SHAM mice, were found in the same quadrant, clustered separately, but closer to each other than to CR and FMT mice (an overview of all relative gene expression changes is shown in Suppl. Table 5 and the corresponding PCA is shown in Suppl. Fig. 1). To validate the qPCR array results, we examined the expression of selected genes by single RT-qPCR and, as shown in Suppl. Fig. 2, the results confirmed the qPCR array expression data for all the examined genes.

16S Metagenomics analyses show that a gut microbiome was reintroduced in GF mice following FMT

Metataxonomic profiling of GF mice subjected to FMT using microbiota samples from CR mice showed an overall microbiome composition very similar to that of CR mice for colon, cecum, ileum and jejunum (Fig. 6A). However, specific taxa were associated to compositional differences, as R-squared of permanova analysis was 45.7% for colon and 30.2% for cecum. Statistical comparison of FMT mice to CR mice for cecum and colon shows that some taxa were differentially abundant between the two groups. *Bacteroidaceae* and *Akkermansiaceae* and *Peptococcaceae* were significantly were increased in the FMT group (Fig. 6B). In opposition, *Lachnospiraceae* were reduced in the FMT group for colon and cecum and *Christensenellaceae* were significantly reduced in FMT group in cecum only.

Discussion

The present study demonstrates that GF mice exhibit significant modifications in eCBome gene expression and mediator levels in the large and, particularly, small intestine of young and adult male mice. Many of these modifications seem to be directly due to the lack of microbiota, since the successful transplantation of intestinal microbiota from donor to age-matched GF mice resulted, after only one week, in the partial or complete reversal of many of these changes. These results are unique and important since they provide a cause-effect relationship between the presence or absence of intestinal microbes, especially those that were successfully reintroduced in GF mice by FMT, and eCBome signaling. Based on the known intestinal functions of eCBome receptors and their endogenous ligands that were altered in GF mice (Table 1), our findings represent the basis for future studies aimed at investigating whether or not such alterations may explain part of the peculiar intestinal phenotype of these mice.

The significant increase in the expression levels of *Cnr1* in 13wk old GF mice that we observed in the ileum and colon, along with the trends towards increases in 2-AG levels in the former and AEA levels in the latter tissue, and together with previous studies showing that activation of the receptor encoded by this gene inhibits intestinal motility and secretion (38–40), may explain in part why these functions are inhibited in GF mice (14). Our results in GF C57BL/6NTac recapitulate those obtained by Muccioli *et. al* in GF Swiss Webster mice, in which *Cnr1* expression was similarly increased in the colon, while a non-significant decrease was observed in the jejunum (19). However, the effect of FMT on these alterations was not investigated. Now we report that FMT partially reversed the increased *Cnr1* expression in the ileum, and fully reversed it, but not selectively over SHAM treatment, in the colon. These data support the notion that microbiota directly regulate *Cnr1* expression in the intestines of mice.

Contrary to *Cnr1*, the expression of the gene encoding for the recently proposed endocannabinoid and plant cannabinoid receptor, GPR55, was significantly decreased in GF mice in all three small intestinal segments analyzed and, except for the jejunum, in both young and adult mice. This effect was reversed by FMT fully and selectively over SHAM treatment in the duodenum, fully but not completely selectively in the jejunum, and partly and selectively in the ileum. Since a similarity between GF C57BL/6NTac and 7wk old Swiss Webster mice was observed (and discussed above) for *Cnr1* (19), we sought to confirm the *Gpr55* expression results in this latter strain, where indeed the GF status resulted again in decreased expression in the ileum and,

not significantly, in the jejunum (the duodenum was not analyzed). GF Swiss Webster mice also presented reduced *Gpr55* expression in the colon, similar to the non-statistically significant trend observed in GF C57BL/6NTac mice at 4 but not 13wk. The reason for this difference may lie in the genetic and age differences between the mice used to perform the experiments. Importantly, however, also in GF Swiss Webster mice gut microbiome conventionalization resulted in rescued *Gpr55* expression. Furthermore, antibiotic treatment of C57BL/6J mice also reduced *Gpr55* mRNA expression in the ileum and, as a non-statistically significant trend, the jejunum and colon. These results, taken together, clearly indicate that the gut microbiome as a whole positively controls the expression of *Gpr55*, particularly in the ileum. The involvement of this receptor in the physiology and pathophysiology of the rodent gut have been described (41), although the description of tissues and cell types expressing this receptor is still lacking. The higher expression of G*pr55* in rats treated with LPS suggested a potential pro-inflammatory role of this receptor in the gut. Thus, decreased GPR55 signaling in the small intestine could be one of the mechanisms underlying decreased gut inflammation in GF mice (42). Future experiments, which are beyond the scope of this study, are needed to address the role of reduced GPR55 signaling in the GF mouse small intestine.

Similar to *Gpr55*, we observed a robust and general decrease in the expression levels of *Gpr18* in the small intestine in GF mice of both ages, an effect that FMT could reverse specifically over SHAM treatment in almost all analyzed parts of this organ. This, in the absence of any significant change in the levels of the proposed ligand for this receptor, i.e. *N*-arachidonoyl-glycine (which was below detection levels of 5 fmol), suggests that the tonic activity of GPR18 may be correspondingly decreased in GF mice. This receptor is required cell-intrinsically for the reconstitution of small intestine intraepithelial lymphocyte subsets (43), whose functionality in inflammatory bowel disease is altered in conjunction with dysbiosis (44). Thus, decreased GPR18 tone in GF mice may influence small intestine inflammatory responses by altering intraepithelial lymphocyte activity.

GF mice exhibit a lean phenotype due to increased energy expenditure, and hence consume more food than controls to maintain the same body weight (45) and are resistant to diet-induced obesity and insulin resistance, showing decreased adiposity and hepatic triglyceride levels (46, 47). Although the underlying mechanisms are still to be elucidated, it is known that GF mice have increased fatty acid oxidation and decreased lipogenesis

(48–50). In our study, we found an increase in the expression levels of the gene encoding the nuclear receptor PPARα in all the tracts of the small intestine and particularly in the duodenum and ileum of both young and adult GF mice; these changes were totally reversed one week after FMT, again specifically over SHAM treatment. PPARα is well known to play an important role in several metabolic pathways and in particular in lipid metabolism, promoting fatty acid oxidation, lipid transport and also ketogenesis and gluconeogenesis (51). Although few reports exist about the role of PPARα in the intestine, the activation of this receptor by OEA in the jejunum was shown to inhibit the intake of dietary fats (52). In accordance with these data, a recent study demonstrated that mice lacking intestinal epithelial *Napepld*, the enzyme mainly responsible of the synthesis of NAEs, display a lower levels of OEA and an increase of lipid absorption and fat mass gain leading to an HFD-induced fatty liver, thus highlighting the importance of the intestinal NAEs in the regulation of the energy homeostasis and to the disruption of signaling leading to the development of obesity and hepatic steatosis (27). We hypothesize that the FMT-reversible increased expression of this nuclear receptor in GF mice could, on the one hand, support the "positive" metabolic phenotype of the GF mice, and, on the other hand, represent an adaptive response counteracting the increased food intake displayed by these mice.

Indeed, increased *Pparα* expression was sustained by, and possibly due to, the simultaneous FMT-reversible increases in the levels of the potent endogenous PPARα agonist OEA, at least in the duodenum of 13wk old GF mice. Other mediators were also found to be increased in some sections of the small intestine, and then decreased back to control levels by FMT. These included the OEA congener, LEA, which, like OEA, acts as a GPR119 agonist (53). GPR119 is a major intestinal stimulator of GLP1 release, which up-regulates insulin and down-regulates glucagon levels and thus control glucose homeostasis, including in response to OEA (54). Interestingly, Wichmann *et al* showed that GF mice are characterized by a 3-fold increase in GLP-1 production, contributing to a better glucose tolerance, while FMT completely abolished the increased GLP-1 production and colonic L-cell number (15). Hence, it is tempting to speculate from our data that increased OEA and LEA may regulate the production of endogenous GLP-1 in GF mice and contribute to their resistance to high fat diet-induced glucose intolerance. Finally, long chain NAEs, such as OEA and LEA, also activate TRPV1 channels (55, 56), which were shown to inhibit food-intake, stimulate insulin sensitivity and release and exert both pro- and anti-inflammatory effects (the latter especially following ligand-induced desensitization) (57).

Importantly, neither GPR119 nor TRPV1 were found here to be affected by lack of the intestinal microbiota (Suppl. Table 5).

Two major genes encoding for enzymes for NAE hydrolysis, i.e. *Faah* and *Naaa*, showed an FMT-reversible increase along all the small intestinal tracts. However, NAE concentrations were not significantly reduced in GF mouse intestinal tissues. This could be due to the fact that also genes encoding NAE anabolic enzymes, i.e. *Abhd4* and, especially, *Gde1*, exhibited increased expression in GF mice, thus possibly counteracting the effects of increased degradation, and even underlying the increase of select NAEs such as OEA and LEA. On the other hand, there was a decrease in the expression of the gene encoding for a potential AEA biosynthetic enzyme, *Ptpn22* (32). However, only scant evidence exists for its involvement in the biosynthesis of NAEs other than AEA, which, as such or through some of its polymorphisms, is instead implicated in intestinal inflammation in a manner dependent on the gut microbiota (58).

Interestingly, two eCBome genes that are more marginally involved in NAE biosynthesis or degradation were instead strongly affected by the lack of microbiota in GF mice. *Ptges*, encoding for prostaglandin E synthase, an enzyme involved in the biosynthesis of PGE_2 but also in the transformation of AEA or 2-AG into prostamide E_2 and prostaglandin glycerol ester E_2 (59, 60) (which, with our method, were below the detection limit of 5 and 25 fmol, respectively), and, even more dramatically, *Pla2g5*, encoding for a calcium-dependent secretory PLA2 catalyzing the release of AA from membrane phospholipids (60), were significantly down-regulated in all tracts of the small and large intestine, in both young and adult mice and in a manner significantly reversed by FMT. For some of these "multi-task" enzymes we hypothesize their involvement in the altered immune response of GF mice, which may be related to decreased pro-inflammatory eicosanoid production.

Regarding the anabolic enzymes for 2-acyl-glycerols, both *Dagla* and *Daglb* were reduced, in a manner reversed by FMT, in young and adult GF mice in the ileum, and, in the case of the latter enzyme, also in jejunum and colon, despite the observed elevation of 2-AG and of 2-EPG levels in this tissue. Intriguingly, the expression of the gene encoding what is considered the second most important enzyme for 2-AG hydrolysis, *Abhd6*, was instead increased in the ileum (as well as in the duodenum and jejunum, and decreased in the colon), in an FMT-reversible manner, again in apparent disagreement with the increases observed with some 2-acyl-glycerols. Among the observed alterations in anabolic or catabolic genes, the latter effect could be due

to the reduction in the expression of *Ppt1*, encoding an enzyme that, however, was shown so far to be involved in 2-AG degradation in only one study (35). In summary, the alterations in monoacylglycerol metabolic enzymes found here in GF mice would have predicted a decrease in the levels of 2-acylglycerols in these mice, and therefore do not seem to account for the increases observed for some members of this lipid family in some intestinal segments.

The fact that the modifications of the eCBome anabolic and catabolic enzyme expression do not necessarily correlate with the changes observed in lipid mediators (when these latter could be/were measured), may be justified by the redundancy of the metabolic pathways and enzymes able to synthesize and degrade these molecules. This redundancy does not always allow for the prediction of changes in metabolic product concentrations based on changes on enzyme expression (61). A further complication derives from the possibility that the concentrations of these lipid mediators are regulated also by the availability of their ultimate phospholipid precursors (34). Thus, the expression of genes encoding for enzymes may also represent adaptive responses to feedback on mediator changes. Finally, the observed alterations in enzyme expression may have impacted upon the concentrations of mediators that we did not measure, such as, for example, the fatty acid primary amides. These bioactive mediators are produced from the action of the enzyme PAM, whose gene we found here to be significantly upregulated in the jejunum and ileum of both young and adult GF mice and sham controls.

Regardless of their role, or lack thereof, in contributing to the gut phenotype or intestinal eCBome mediator levels, the observed mRNA expression levels of eCBome receptors or metabolic enzymes in GF and SHAM mice, one the one hand, and CR and FMT mice, on the other hand, overall clustered together or very close in PCA analyses, at least in the small intestine, where most of the FMT-induced reversals were observed. This observation, together with our metagenomics data showing that the FMT did indeed restore in GF mice a gut bacterial population very similar to that found in CR mice, reinforces the hypothesis of a direct link between the gut microbiota and the eCBome, at least in this part of the gut. This hypothesis is supported also by previous findings by Everard et al. (62, 63) showing that: 1) mice lacking, specifically in intestinal epithelial cells, the key toll-like receptor adaptor protein MyD88, which mediates some of the systemic inflammatory effects of gut microbiota-derived lipopolysaccharides, and 2) wild type mice under a high fat diet treated with the

metabolically beneficial commensal bacterium, *Akkermansia muciniphila*, both exhibit higher intestinal levels of eCBome mediators with anti-inflammatory and GLP-1 stimulating effects.

In conclusion, we showed here that GF mice, starting at 4 weeks and until at least 13 weeks of age, undergo important changes in eCBome signaling that a partial introduction of the intestinal microbiota is able to reverse after only one week. These findings provide unprecedented direct evidence of how the eCBome in the small intestine is subject to regulation by commensal microorganisms. Further studies are now needed to investigate if the changes observed here are responsible for some of the intestinal phenotypes of GF mice, and to assess if the manipulation of gut microorganisms by different diets and pre-, pro- and sym-biotics or, more selectively, with antibiotics and bacteriophages, may impact on the eCBome and, hence, the physiopathological conditions in which this complex signaling system is involved.

Acknowledgements

We thank Dr. Francesco Tinto for the synthesis of the standard lipid mediator *N*-oleoyl-L-serine, Cynthia Faubert as the responsible for the GF facility at IUCPQ, Dr. Dominique Boudreau for his helpfulness in the quality control of the samples for the 16S analysis and all the colleagues, particularly Mélissa Shen, of Prof. Cristoforo Silvestri team for their help. This study was supported by the Canada Research Excellence Chair in the Microbiome-Endocannabinoidome Axis in Metabolic Health (CERC-MEND), which is funded by the Tri-Agency of the Canadian Federal Government (The Canadian Institutes of Health Research (CIHR), the Natural Sciences and Engineering Research Council of Canada (NSERC), and the Social Sciences and Humanities Research Council of Canada (SSHRC), to Vincenzo Di Marzo, as well as by the Canadian Foundation of Innovation (to Vincenzo Di Marzo) and the Sentinelle Nord-Apogée program (to Université Laval). Claudia Manca received a post-doctoral grant from the Joint International Research Unit for Chemical and Biomolecular Research on the Microbiome and its impact on Metabolic Health and Nutrition (UMI-MicroMeNu), which is supported by the Sentinelle Nord program. Computing was performed on Compute Canada infrastructure (RRG2734).

Patrice D. Cani is a senior research associate at FRS-FNRS (Fonds de la Recherche Scientifique), Belgium. This work was supported by the Fonds Baillet Latour (Grant for Medical Research 2015), the Fonds de la Recherche Scientifique (FNRS FRFS-WELBIO: WELBIO-CR-2019C-02R) and ERC Starting Grant 2013 (336452-ENIGMO).

References

1. Mazidi, M., P. Rezaie, A. P. Kengne, M. G. Mobarhan, and G. A. Ferns. 2016. Gut microbiome and metabolic syndrome. *Diabetes & Metabolic Syndrome: Clinical Research & Reviews*. **10**: S150–S157.

2. Clemente, J. C., L. K. Ursell, L. W. Parfrey, and R. Knight. 2012. The Impact of the Gut Microbiota on Human Health: An Integrative View. *Cell*. **148**: 1258–1270.

3. Jandhyala, S. M. 2015. Role of the normal gut microbiota. *World Journal of Gastroenterology*. **21**: 8787.

4. Al-Asmakh, M., F. Anuar, F. Zadjali, J. Rafter, and S. Pettersson. 2012. Gut microbial communities modulating brain development and function. *Gut Microbes*. **3**: 366–373.

5. Nicholson, J. K., E. Holmes, J. Kinross, R. Burcelin, G. Gibson, W. Jia, and S. Pettersson. 2012. Host-gut microbiota metabolic interactions. *Science*. **336**: 1262–1267.

6. Björkholm, B., C. M. Bok, A. Lundin, J. Rafter, M. L. Hibberd, and S. Pettersson. 2009. Intestinal Microbiota Regulate Xenobiotic Metabolism in the Liver. *PLOS ONE*. **4**: e6958.

7. Ringel, Y., N. Maharshak, T. Ringel-Kulka, E. A. Wolber, R. B. Sartor, and I. M. Carroll. 2015. High throughput sequencing reveals distinct microbial populations within the mucosal and luminal niches in healthy individuals. *Gut Microbes*. **6**: 173–181.

8. Pédron, T., C. Mulet, C. Dauga, L. Frangeul, C. Chervaux, G. Grompone, and P. J. Sansonetti. 2012. A Crypt-Specific Core Microbiota Resides in the Mouse Colon. *mBio*. **3**. [online] https://mbio.asm.org/lookup/doi/10.1128/mBio.00116-12 (Accessed June 23, 2019).

9. Goodrich, J. K., J. L. Waters, A. C. Poole, J. L. Sutter, O. Koren, R. Blekhman, M. Beaumont, W. Van Treuren, R. Knight, J. T. Bell, T. D. Spector, A. G. Clark, and R. E. Ley. 2014. Human genetics shape the gut microbiome. *Cell*. **159**: 789–799.

10. Hopkins, M., R. Sharp, and G. Macfarlane. 2001. Age and disease related changes in intestinal bacterial populations assessed by cell culture, 16S rRNA abundance, and community cellular fatty acid profiles. *Gut*. **48**: 198–205.

11. Martínez, I., J. C. Stegen, M. X. Maldonado-Gómez, A. M. Eren, P. M. Siba, A. R. Greenhill, and J. Walter. 2015. The gut microbiota of rural papua new guineans: composition, diversity patterns, and ecological processes. *Cell Rep*. **11**: 527–538.

12. Al-Asmakh, M., and F. Zadjali. 2015. Use of Germ-Free Animal Models in Microbiota-Related Research. *J. Microbiol. Biotechnol.* **25**: 1583–1588.

13. Round, J. L., and S. K. Mazmanian. 2009. The gut microbiome shapes intestinal immune responses during health and disease. *Nat Rev Immunol*. **9**: 313–323.

14. Husebye, E., P. M. Hellström, F. Sundler, J. Chen, and T. Midtvedt. 2001. Influence of microbial species on small intestinal myoelectric activity and transit in germ-free rats. *Am. J. Physiol. Gastrointest. Liver Physiol.* **280**: G368-380.

15. Wichmann, A., A. Allahyar, T. U. Greiner, H. Plovier, G. Ö. Lundén, T. Larsson, D. J. Drucker, N. M. Delzenne, P. D. Cani, and F. Bäckhed. 2013. Microbial Modulation of Energy Availability in the Colon Regulates Intestinal Transit. *Cell Host & Microbe*. **14**: 582–590.

16. Akira, S., and H. Hemmi. 2003. Recognition of pathogen-associated molecular patterns by TLR family. *Immunol. Lett.* **85**: 85–95.

17. Macpherson, A. J., and N. L. Harris. 2004. Interactions between commensal intestinal bacteria and the immune system. *Nat. Rev. Immunol.* **4**: 478–485.

18. Cani, P. D., J. Amar, M. A. Iglesias, M. Poggi, C. Knauf, D. Bastelica, A. M. Neyrinck, F. Fava, K. M. Tuohy, C. Chabo, A. Waget, E. Delmée, B. Cousin, T. Sulpice, B. Chamontin, J. Ferrières, J.-F. Tanti, G. R. Gibson, L. Casteilla, N. M. Delzenne, M. C. Alessi, and R. Burcelin. 2007. Metabolic endotoxemia initiates obesity and insulin resistance. *Diabetes*. **56**: 1761–1772.

19. Muccioli, G. G., D. Naslain, F. Bäckhed, C. S. Reigstad, D. M. Lambert, N. M. Delzenne, and P. D. Cani. 2010. The endocannabinoid system links gut microbiota to adipogenesis. *Mol. Syst. Biol.* **6**: 392.

20. Di Marzo Vincenzo, and De Petrocellis Luciano. 2012. Why do cannabinoid receptors have more than one endogenous ligand? *Philosophical Transactions of the Royal Society B: Biological Sciences*. **367**: 3216–3228.

21. The Endocannabinoidome - 1st Edition. [online] https://www.elsevier.com/books/the-endocannabinoidome/di-marzo/978-0-12-420126-2 (Accessed June 26, 2019).

22. Di Marzo, V. 2018. New approaches and challenges to targeting the endocannabinoid system. *Nat Rev Drug Discov*. **17**: 623–639.

23. Piscitelli, F., and V. Di Marzo. 2015. *In* Cannabinoids in Neurologic and Mental Disease (Fattore, L., ed.). pp. xxv–xlv. , Academic Press, San Diego. [online] http://www.sciencedirect.com/science/article/pii/B9780124170414000242 (Accessed June 26, 2019).

24. Massa, F., and K. Monory. 2006. Endocannabinoids and the gastrointestinal tract. *J. Endocrinol. Invest.* **29**: 47–57.

25. Guida, F., F. Turco, M. Iannotta, D. De Gregorio, I. Palumbo, G. Sarnelli, A. Furiano, F. Napolitano, S. Boccella, L. Luongo, M. Mazzitelli, A. Usiello, F. De Filippis, F. A. Iannotti, F. Piscitelli, D. Ercolini, V. de Novellis, V. Di Marzo, R. Cuomo, and S. Maione. 2018. Antibiotic-induced microbiota perturbation causes gut endocannabinoidome changes, hippocampal neuroglial reorganization and depression in mice. *Brain Behav. Immun.* **67**: 230–245.

26. Adipose tissue NAPE-PLD controls fat mass development by altering the browning process and gut microbiota | Nature Communications. [online] https://www-nature-com.acces.bibl.ulaval.ca/articles/ncomms7495 (Accessed June 23, 2019).

27. Everard, A., H. Plovier, M. Rastelli, M. V. Hul, A. de W. d'Oplinter, L. Geurts, C. Druart, S. Robine, N. M. Delzenne, G. G. Muccioli, W. M. de Vos, S. Luquet, N. Flamand, V. D. Marzo, and P. D. Cani. 2019. Intestinal epithelial N -acylphosphatidylethanolamine phospholipase D links dietary fat to metabolic adaptations in obesity and steatosis. *Nature Communications*. **10**: 457.

28. Bligh, E. G., and W. J. Dyer. 1959. A rapid method of total lipid extraction and purification. *Can. J. Biochem. Physiol*. **37**: 911–917.

29. Josse, J., and F. Husson. 2016. missMDA: A Package for Handling Missing Values in Multivariate Data Analysis. *Journal of Statistical Software*. **70**: 1–31.

30. Callahan, B. J., P. J. McMurdie, M. J. Rosen, A. W. Han, A. J. A. Johnson, and S. P. Holmes. 2016. DADA2: High-resolution sample inference from Illumina amplicon data. *Nature Methods*. **13**: 581–583.

31. Anderson, M. J. 2017. *In* Wiley StatsRef: Statistics Reference Online. pp. 1–15. , American Cancer Society. [online] http://onlinelibrary.wiley.com/doi/abs/10.1002/9781118445112.stat07841 (Accessed June 26, 2019).

32. Liu, J., L. Wang, J. Harvey-White, D. Osei-Hyiaman, R. Razdan, Q. Gong, A. C. Chan, Z. Zhou, B. X. Huang, H.-Y. Kim, and G. Kunos. 2006. A biosynthetic pathway for anandamide. *PNAS*. **103**: 13345–13350.

33. Bisogno, T., F. Howell, G. Williams, A. Minassi, M. G. Cascio, A. Ligresti, I. Matias, A. Schiano-Moriello, P. Paul, E.-J. Williams, U. Gangadharan, C. Hobbs, V. D. Marzo, and P. Doherty. 2003. Cloning of the first sn1-DAG lipases points to the spatial and temporal regulation of endocannabinoid signaling in the brain. *J Cell Biol*. **163**: 463–468.

34. Di Marzo, V. 2008. *In* Reviews of Physiology Biochemistry and Pharmacology Reviews of Physiology, Biochemistry and Pharmacology (Amara, S. G., Bamberg, E., Fleischmann, B., Gudermann, T., Hebert, S. C., Jahn, R., Lederer, W. J., Lill, R., Miyajima, A., Offermanns, S.,

and Zechner, R., eds.). pp. 1–24. , Springer Berlin Heidelberg, Berlin, Heidelberg. [online] https://doi.org/10.1007/112_0505 (Accessed June 23, 2019).

35. Wang, R., A. Borazjani, A. T. Matthews, L. C. Mangum, M. J. Edelmann, and M. K. Ross. 2013. Identification of palmitoyl protein thioesterase 1 in human THP-1 monocytes/macrophages and characterization of unique biochemical activities for this enzyme. *Biochemistry*. **52**: 7559–7574.

36. Marrs, W. R., J. L. Blankman, E. A. Horne, A. Thomazeau, Y. H. Lin, J. Coy, A. L. Bodor, G. G. Muccioli, S. S.-J. Hu, G. Woodruff, S. Fung, M. Lafourcade, J. P. Alexander, J. Z. Long, W. Li, C. Xu, T. Möller, K. Mackie, O. J. Manzoni, B. F. Cravatt, and N. Stella. 2010. The serine hydrolase ABHD6 controls the accumulation and efficacy of 2-AG at cannabinoid receptors. *Nat Neurosci*. **13**: 951–957.

37. Navia-Paldanius, D., J. R. Savinainen, and J. T. Laitinen. 2012. Biochemical and pharmacological characterization of human α/β-hydrolase domain containing 6 (ABHD6) and 12 (ABHD12). *J Lipid Res*. **53**: 2413–2424.

38. Pinto, L., A. A. Izzo, M. G. Cascio, T. Bisogno, K. Hospodar-Scott, D. R. Brown, N. Mascolo, V. Di Marzo, and F. Capasso. 2002. Endocannabinoids as physiological regulators of colonic propulsion in mice. *Gastroenterology*. **123**: 227–234.

39. Izzo, A. A., F. Capasso, A. Costagliola, T. Bisogno, G. Marsicano, A. Ligresti, I. Matias, R. Capasso, L. Pinto, F. Borrelli, A. Cecio, B. Lutz, N. Mascolo, and V. Di Marzo. 2003. An endogenous cannabinoid tone attenuates cholera toxin-induced fluid accumulation in mice. *Gastroenterology*. **125**: 765–774.

40. Izzo, A. A., F. Fezza, R. Capasso, T. Bisogno, L. Pinto, T. Iuvone, G. Esposito, N. Mascolo, V. Di Marzo, and F. Capasso. 2001. Cannabinoid CB1-receptor mediated regulation of gastrointestinal motility in mice in a model of intestinal inflammation. *Br. J. Pharmacol.* **134**: 563–570.

41. Schicho, R., and M. Storr. 2012. A potential role for GPR55 in gastrointestinal functions. *Current Opinion in Pharmacology*. **12**: 653–658.

42. Hernández-Chirlaque, C., C. J. Aranda, B. Ocón, F. Capitán-Cañadas, M. Ortega-González, J. J. Carrero, M. D. Suárez, A. Zarzuelo, F. Sánchez de Medina, and O. Martínez-Augustin. 2016. Germ-free and Antibiotic-treated Mice are Highly Susceptible to Epithelial Injury in DSS Colitis. *J Crohns Colitis*. **10**: 1324–1335.

43. Wang, X., H. Sumida, and J. G. Cyster. 2014. GPR18 is required for a normal CD8αα intestinal intraepithelial lymphocyte compartment. *Journal of Experimental Medicine*. **211**: 2351–2359.

44. Regner, E. H., N. Ohri, A. Stahly, M. E. Gerich, B. P. Fennimore, D. Ir, W. K. Jubair, C. Görg, J. Siebert, C. E. Robertson, L. Caplan, D. N. Frank, and K. A. Kuhn. 2018. Functional intraepithelial lymphocyte changes in inflammatory bowel disease and spondyloarthritis have disease specific correlations with intestinal microbiota. *Arthritis Res Ther*. **20**. [online] https://www.ncbi.nlm.nih.gov/pmc/articles/PMC6053728/ (Accessed June 23, 2019).

45. Wostmann, B. S., C. Larkin, A. Moriarty, and E. Bruckner-Kardoss. 1983. Dietary intake, energy metabolism, and excretory losses of adult male germfree Wistar rats. *Lab. Anim. Sci.* **33**: 46–50.

46. Bäckhed, F., J. K. Manchester, C. F. Semenkovich, and J. I. Gordon. 2007. Mechanisms underlying the resistance to diet-induced obesity in germ-free mice. *Proc Natl Acad Sci U S A*. **104**: 979–984.

47. Khan, M. J., K. Gerasimidis, C. A. Edwards, and M. G. Shaikh. 2016. Role of Gut Microbiota in the Aetiology of Obesity: Proposed Mechanisms and Review of the Literature. *J Obes*. **2016**. [online] https://www.ncbi.nlm.nih.gov/pmc/articles/PMC5040794/ (Accessed June 23, 2019).

48. Bäckhed, F., H. Ding, T. Wang, L. V. Hooper, G. Y. Koh, A. Nagy, C. F. Semenkovich, and J. I. Gordon. 2004. The gut microbiota as an environmental factor that regulates fat storage. *PNAS*. **101**: 15718–15723.

49. Bäckhed, F., J. K. Manchester, C. F. Semenkovich, and J. I. Gordon. 2007. Mechanisms underlying the resistance to diet-induced obesity in germ-free mice. *Proc. Natl. Acad. Sci. U.S.A.* **104**: 979–984.

50. Velagapudi, V. R., R. Hezaveh, C. S. Reigstad, P. Gopalacharyulu, L. Yetukuri, S. Islam, J. Felin, R. Perkins, J. Borén, M. Orešič, and F. Bäckhed. 2010. The gut microbiota modulates host energy and lipid metabolism in mice. *J. Lipid Res.* **51**: 1101–1112.

51. Reddy, J. K., and T. Hashimoto. 2001. Peroxisomal beta-oxidation and peroxisome proliferator-activated receptor alpha: an adaptive metabolic system. *Annu. Rev. Nutr.* **21**: 193–230.

52. Schwartz, G. J., J. Fu, G. Astarita, X. Li, S. Gaetani, P. Campolongo, V. Cuomo, and D. Piomelli. 2008. The lipid messenger OEA links dietary fat intake to satiety. *Cell Metab*. **8**: 281–288.

53. Syed, S. K., H. H. Bui, L. S. Beavers, T. B. Farb, J. Ficorilli, A. K. Chesterfield, M.-S. Kuo, K. Bokvist, D. G. Barrett, and A. M. Efanov. 2012. Regulation of GPR119 receptor activity with endocannabinoid-like lipids. *American Journal of Physiology-Endocrinology and Metabolism*. **303**: E1469–E1478.

54. Lauffer, L. M., R. Iakoubov, and P. L. Brubaker. 2009. GPR119 is essential for oleoylethanolamide-induced glucagon-like peptide-1 secretion from the intestinal enteroendocrine L-cell. *Diabetes*. **58**: 1058–1066.

55. Raboune, S., J. M. Stuart, E. Leishman, S. M. Takacs, B. Rhodes, A. Basnet, E. Jameyfield, D. McHugh, T. Widlanski, and H. B. Bradshaw. 2014. Novel endogenous N-acyl amides activate TRPV1-4 receptors, BV-2 microglia, and are regulated in brain in an acute model of inflammation. *Front Cell Neurosci*. **8**: 195.

56. De Petrocellis, L., M. Nabissi, G. Santoni, and A. Ligresti. 2017. Actions and Regulation of Ionotropic Cannabinoid Receptors. *Adv. Pharmacol.* **80**: 249–289.

57. Christie, S., G. A. Wittert, H. Li, and A. J. Page. 2018. Involvement of TRPV1 Channels in Energy Homeostasis. *Front. Endocrinol.* **9**. [online]

https://www.frontiersin.org/articles/10.3389/fendo.2018.00420/full (Accessed August 24, 2019).

58. Pike, K. A., and M. L. Tremblay. 2018. Protein Tyrosine Phosphatases: Regulators of CD4 T Cells in Inflammatory Bowel Disease. *Front Immunol*. **9**. [online] https://www.ncbi.nlm.nih.gov/pmc/articles/PMC6220082/ (Accessed June 23, 2019).

59. Matias, I., J. Chen, L. D. Petrocellis, T. Bisogno, A. Ligresti, F. Fezza, A. H.-P. Krauss, L. Shi, C. E. Protzman, C. Li, Y. Liang, A. L. Nieves, K. M. Kedzie, R. M. Burk, V. D. Marzo, and D. F. Woodward. 2004. Prostaglandin Ethanolamides (Prostamides): In Vitro Pharmacology and Metabolism. *J Pharmacol Exp Ther*. **309**: 745–757.

60. Astudillo, A. M., M. A. Balboa, and J. Balsinde. 2019. Selectivity of phospholipid hydrolysis by phospholipase A2 enzymes in activated cells leading to polyunsaturated fatty acid mobilization. *Biochimica et Biophysica Acta (BBA) - Molecular and Cell Biology of Lipids*. **1864**: 772–783.

61. "Redundancy" of Endocannabinoid Inactivation: New Challenges and Opportunities for Pain Control | ACS Chemical Neuroscience. [online] https://pubs-acs-org.acces.bibl.ulaval.ca/doi/abs/10.1021/cn300015x (Accessed June 23, 2019).

62. Everard, A., L. Geurts, R. Caesar, M. Van Hul, S. Matamoros, T. Duparc, R. G. P. Denis, P. Cochez, F. Pierard, J. Castel, L. B. Bindels, H. Plovier, S. Robine, G. G. Muccioli, J.-C. Renauld, L. Dumoutier, N. M. Delzenne, S. Luquet, F. Bäckhed, and P. D. Cani. 2014. Intestinal epithelial MyD88 is a sensor switching host metabolism towards obesity according to nutritional status. *Nature Communications*. **5**: 5648.

63. Everard, A., C. Belzer, L. Geurts, J. P. Ouwerkerk, C. Druart, L. B. Bindels, Y. Guiot, M. Derrien, G. G. Muccioli, N. M. Delzenne, W. M. de Vos, and P. D. Cani. 2013. Cross-talk between Akkermansia muciniphila and intestinal epithelium controls diet-induced obesity. *PNAS*. **110**: 9066–9071.

64. Sugiura, T., S. Kondo, A. Sukagawa, S. Nakane, A. Shinoda, K. Itoh, A. Yamashita, and K. Waku. 1995. 2-Arachidonoylglycerol: a possible endogenous cannabinoid receptor ligand in brain. *Biochem. Biophys. Res. Commun.* **215**: 89–97.

65. Sugiura, T., T. Kodaka, S. Nakane, T. Miyashita, S. Kondo, Y. Suhara, H. Takayama, K. Waku, C. Seki, N. Baba, and Y. Ishima. 1999. Evidence That the Cannabinoid CB1 Receptor Is a 2-Arachidonoylglycerol Receptor STRUCTURE-ACTIVITY RELATIONSHIP OF 2-ARACHIDONOYLGLYCEROL, ETHER-LINKED ANALOGUES, AND RELATED COMPOUNDS. *J. Biol. Chem.* **274**: 2794–2801.

66. Thakur, G. A., S. P. Nikas, and A. Makriyannis. 2005. CB1 cannabinoid receptor ligands. *Mini Rev Med Chem*. **5**: 631–640.

67. Cluny, N. L., C. M. Keenan, M. Duncan, A. Fox, B. Lutz, and K. A. Sharkey. 2010. Naphthalen-1-yl-(4-pentyloxynaphthalen-1-yl)methanone (SAB378), a peripherally restricted cannabinoid CB1/CB2 receptor agonist, inhibits gastrointestinal motility but has no effect on experimental colitis in mice. *J. Pharmacol. Exp. Ther.* **334**: 973–980.

68. DiPatrizio, N. V., G. Astarita, G. Schwartz, X. Li, and D. Piomelli. 2011. Endocannabinoid signal in the gut controls dietary fat intake. *Proc. Natl. Acad. Sci. U.S.A.* **108**: 12904–12908.

69. Karwad, M. A., D. G. Couch, E. Theophilidou, S. Sarmad, D. A. Barrett, M. Larvin, K. L. Wright, J. N. Lund, and S. E. O'Sullivan. 2017. The role of CB1 in intestinal permeability and inflammation. *FASEB J.* **31**: 3267–3277.

70. Alhamoruni, A., K. L. Wright, M. Larvin, and S. E. O'Sullivan. 2012. Cannabinoids mediate opposing effects on inflammation-induced intestinal permeability. *Br. J. Pharmacol.* **165**: 2598–2610.

71. Grunewald, Z. I., S. Lee, R. Kirkland, M. Ross, and C. B. de La Serre. 2019. Cannabinoid receptor type-1 partially mediates metabolic endotoxemia-induced inflammation and insulin resistance. *Physiol. Behav.* **199**: 282–291.

72. Balvers, M. G. J., K. C. M. Verhoeckx, P. Plastina, H. M. Wortelboer, J. Meijerink, and R. F. Witkamp. 2010. Docosahexaenoic acid and eicosapentaenoic acid are converted by 3T3-L1 adipocytes to N-acyl ethanolamines with anti-inflammatory properties. *Biochim. Biophys. Acta*. **1801**: 1107–1114.

73. Sugiura, T., S. Kondo, S. Kishimoto, T. Miyashita, S. Nakane, T. Kodaka, Y. Suhara, H. Takayama, and K. Waku. 2000. Evidence that 2-arachidonoylglycerol but not N-palmitoylethanolamine or anandamide is the physiological ligand for the cannabinoid CB2 receptor. Comparison of the agonistic activities of various cannabinoid receptor ligands in HL-60 cells. *J. Biol. Chem.* **275**: 605–612.

74. Cannabinoid CB2 receptors in the enteric nervous system modulate gastrointestinal contractility in lipopolysaccharide-treated rats | American Journal of Physiology-Gastrointestinal and Liver Physiology. [online] https://physiology.org/doi/full/10.1152/ajpgi.90285.2008 (Accessed June 23, 2019).

75. Parlar, A., S. O. Arslan, M. F. Doğan, S. A. Çam, A. Yalçin, E. Elibol, M. K. Özer, F. Üçkardeş, and H. Kara. 2018. The exogenous administration of CB2 specific agonist, GW405833, inhibits inflammation by reducing cytokine production and oxidative stress. *Experimental and Therapeutic Medicine*. **16**: 4900–4908.

76. Karwad, M. A., T. Macpherson, B. Wang, E. Theophilidou, S. Sarmad, D. A. Barrett, M. Larvin, K. L. Wright, J. N. Lund, and S. E. O'Sullivan. 2017. Oleoylethanolamine and palmitoylethanolamine modulate intestinal permeability in vitro via TRPV1 and PPARα. *FASEB J.* **31**: 469–481.

77. Lee, E., D. Y. Jung, J. H. Kim, P. R. Patel, X. Hu, Y. Lee, Y. Azuma, H.-F. Wang, N. Tsitsilianos, U. Shafiq, J. Y. Kwon, H. J. Lee, K. W. Lee, and J. K. Kim. 2015. Transient receptor potential vanilloid type-1 channel regulates diet-induced obesity, insulin resistance, and leptin resistance. *FASEB J.* **29**: 3182–3192.

78. Ambrosino, P., M. V. Soldovieri, C. Russo, and M. Taglialatela. 2013. Activation and desensitization of TRPV1 channels in sensory neurons by the PPARα agonist palmitoylethanolamide. *Br. J. Pharmacol.* **168**: 1430–1444.

79. Sagar, D. R., D. A. Kendall, and V. Chapman. 2008. Inhibition of fatty acid amide hydrolase produces PPAR-alpha-mediated analgesia in a rat model of inflammatory pain. *Br. J. Pharmacol.* **155**: 1297–1306.

80. Silveira, L. S., G. D. Pimentel, C. O. Souza, L. A. Biondo, A. A. S. Teixeira, E. A. Lima, H. A. P. Batatinha, J. C. Rosa Neto, and F. S. Lira. 2017. Effect of an acute moderate-exercise session on metabolic and inflammatory profile of PPAR-α knockout mice. *Cell Biochem. Funct.* **35**: 510–517.

81. Pawlak, M., P. Lefebvre, and B. Staels. 2015. Molecular mechanism of PPARα action and its impact on lipid metabolism, inflammation and fibrosis in non-alcoholic fatty liver disease. *J. Hepatol.* **62**: 720–733.

82. Rovito, D., C. Giordano, D. Vizza, P. Plastina, I. Barone, I. Casaburi, M. Lanzino, F. De Amicis, D. Sisci, L. Mauro, S. Aquila, S. Catalano, D. Bonofiglio, and S. Andò. 2013. Omega-3 PUFA ethanolamides DHEA and EPEA induce autophagy through PPARγ activation in MCF-7 breast cancer cells. *J. Cell. Physiol.* **228**: 1314–1322.

83. Bouaboula, M., S. Hilairet, J. Marchand, L. Fajas, G. F. Le, and P. Casellas. 2005. Anandamide induced PPARgamma transcriptional activation and 3T3-L1 preadipocyte differentiation. *Eur J Pharmacol*. **517**: 174–181.

84. Duszka, K., M. Oresic, C. Le May, J. König, and W. Wahli. 2017. PPARγ Modulates Long Chain Fatty Acid Processing in the Intestinal Epithelium. *International Journal of Molecular Sciences*. **18**: 2559.

85. Bassaganya-Riera, J., S. Misyak, A. J. Guri, and R. Hontecillas. 2009. PPAR gamma is highly expressed in F4/80(hi) adipose tissue macrophages and dampens adipose-tissue inflammation. *Cell. Immunol.* **258**: 138–146.

86. Kramar, C., M. Loureiro, J. Renard, and S. R. Laviolette. 2017. Palmitoylethanolamide Modulates GPR55 Receptor Signaling in the Ventral Hippocampus to Regulate Mesolimbic Dopamine Activity, Social Interaction, and Memory Processing. *Cannabis and Cannabinoid Research*. **2**: 8–20.

87. Lin, X.-H., B. Yuece, Y.-Y. Li, Y.-J. Feng, J.-Y. Feng, L.-Y. Yu, K. Li, Y.-N. Li, and M. Storr. 2011. A novel CB receptor GPR55 and its ligands are involved in regulation of gut movement in rodents. *Neurogastroenterol. Motil.* **23**: 862-e342.

88. Stančić, A., K. Jandl, C. Hasenöhrl, F. Reichmann, G. Marsche, R. Schuligoi, A. Heinemann, M. Storr, and R. Schicho. 2015. The GPR55 antagonist CID16020046 protects against intestinal inflammation. *Neurogastroenterol. Motil.* **27**: 1432–1445.

89. Lan, H., H. V. Lin, C. F. Wang, M. J. Wright, S. Xu, L. Kang, K. Juhl, J. A. Hedrick, and T. J. Kowalski. 2012. Agonists at GPR119 mediate secretion of GLP-1 from mouse enteroendocrine cells through glucose-independent pathways. *Br. J. Pharmacol.* **165**: 2799–2807.

90. Hansen, H. S., M. M. Rosenkilde, J. J. Holst, and T. W. Schwartz. 2012. GPR119 as a fat sensor. *Trends Pharmacol. Sci.* **33**: 374–381.

Table 1: Principal features of investigated endocannabinoidome molecular targets and lipid ligands

Most studied eCBome targets	**eCBome mediators that activate the target**	**Role of the target in the small or large intestine**	**Role in inflammation of the target**	**Anabolic or *Catabolic* enzymes reported to regulate the levels of the eCBome mediators, and found to be altered in this study** (22)
CB1	AEA (Ki=61nM), 2-AG (Ki=472nM)>, DHEA (Ki=324nM) (64–66)	↓ Motility (67) ↓ Satiety in response to fat intake (68) ↑ Paracellular permeability (69, 70)	Pro-inflammatory (71)	GDE1, ABHD4, PTPN22 (for NAEs) DAGLα, DAGLβ (for 2-acylglycerols) *FAAH (for NAEs)* *ABHD6, PPT1 (for 2-acylglycerols)*
CB2	2-AG (Ki=1400nM)> AEA (Ki=1930nM) ≥ DHEA (64, 66, 72, 73)	↓ Motility in gut inflammatory states (74)	Anti-inflammatory (75)	GDE1, ABHD4, PTPN22 (for NAEs) DAGLα, DAGLβ (for 2-acylglycerols) *FAAH (for NAEs)* *ABHD6, PPT1 (for 2-acylglycerols)*
TRPV1	Unsaturated and polyunsaturated NAEs and 2-MAGs, including AEA and 2-AG (55, 56)	↓ Paracellular permeability (76) ↑ GLP-1 release (77)	Anti-inflammatory (due to its rapid desensitization) (78)	GDE1, ABHD4, PTPN22 (for NAEs) DAGLα, DAGLβ (for 2-acylglycerols) *FAAH (for NAEs)* *ABHD6, PPT1 (for 2-acylglycerols)*
PPARα	OEA > PEA > DHEA (79)	↑ Satiety in response to fat intake (52) ↓ Paracellular permeability (76)	Anti-inflammatory (80, 81)	GDE1, ABHD4, PTPN22 FAAH, NAAA
PPARγ	AEA, DHEA (82, 83)	↑ Lipid metabolism (84)	Anti-inflammatory (85)	GDE1, ABHD4, PTPN22 FAAH
GPR55	PEA (86)	↓ Motility (87)	Anti-inflammatory (88)	GDE1, ABHD4, PTPN22 NAAA
GPR18	*N*-arachidonoyl-glycine	↑ Correct immune response of the intestine (43)	Possibly anti-inflammatory (44)	FAAH, PAM
GPR119	OEA, LEA, 2-LG, 2-OG (53)	↑ GLP-1 release (89, 90)	unknown	GDE1, ABHD4, PTPN22 (for NAEs) DAGLα, DAGLβ (for 2-acylglycerols) FAAH (for NAEs) ABHD6 (for 2-acylglycerols)

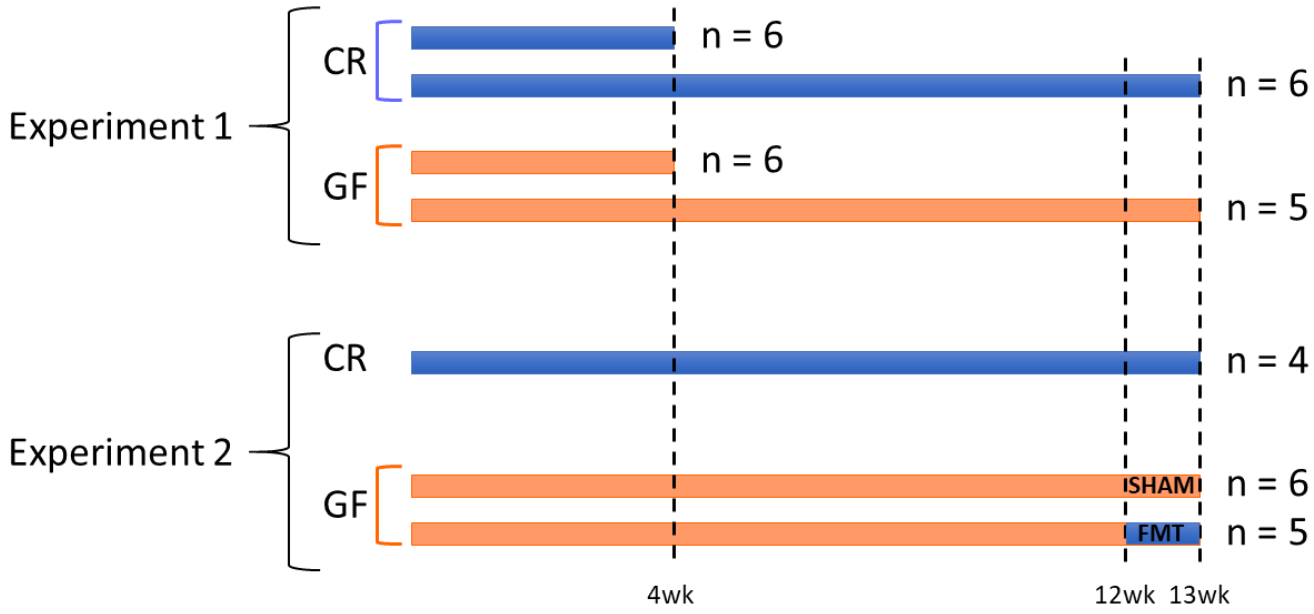

Figure 1. Experimental protocols. **A)** Six male conventionally raised (CR) and germ free (GF) mice were euthanized at 4 and 13wk of age. **B)** For fecal microbiome transfer (FMT), 12wk old GF mice were gavaged with either intestinal contents and stools coming from one and 4 donor mice, respectively (FMT group; n=6) or sterile PBS (SHAM group; n=5). For both experiments, sections of duodenum, jejunum, ileum, cecum and colon were isolated, and the intestinal contents were harvested.

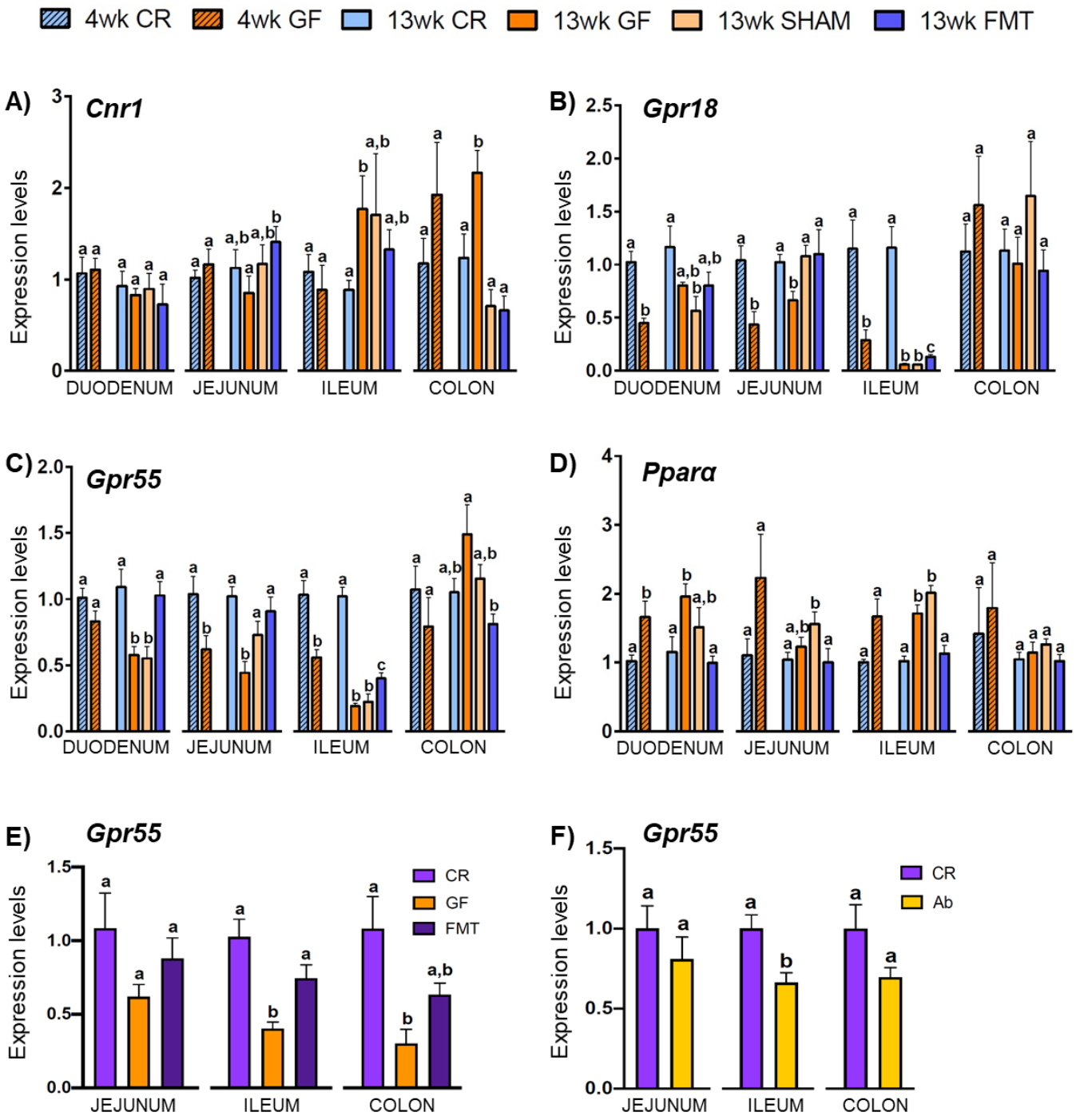

Fig. 2: (A-D) Intestinal expression levels of the eCBome receptors *Cnr1* **(A)**, *Gpr18* **(B)**, *Gpr55* **(C)** and *Pparα* **(D)** in 4 and 13wk old conventionally raised (CR) and germ free (GF) mice and in 13wk male GF mice gavaged with sterile PBS (SHAM) or fecal microbiota (FMT). The mRNA expression levels of were measured by qPCR array in duodenum, jejunum, ileum and colon for all experimental groups and are expressed relative to CR mice for each age within each tissue. Values are mean ± S.E.M. of n=5-10 mice. Bars marked with different letters were significantly different at the p≤0.05 level. **(E-F)** *Gpr55* gene expression in 7wk CR, GF and FMT

Swiss Webster mice **(E)** and control (CT) or antibiotics treated (Ab) C57BL/6J mice **(F)**.

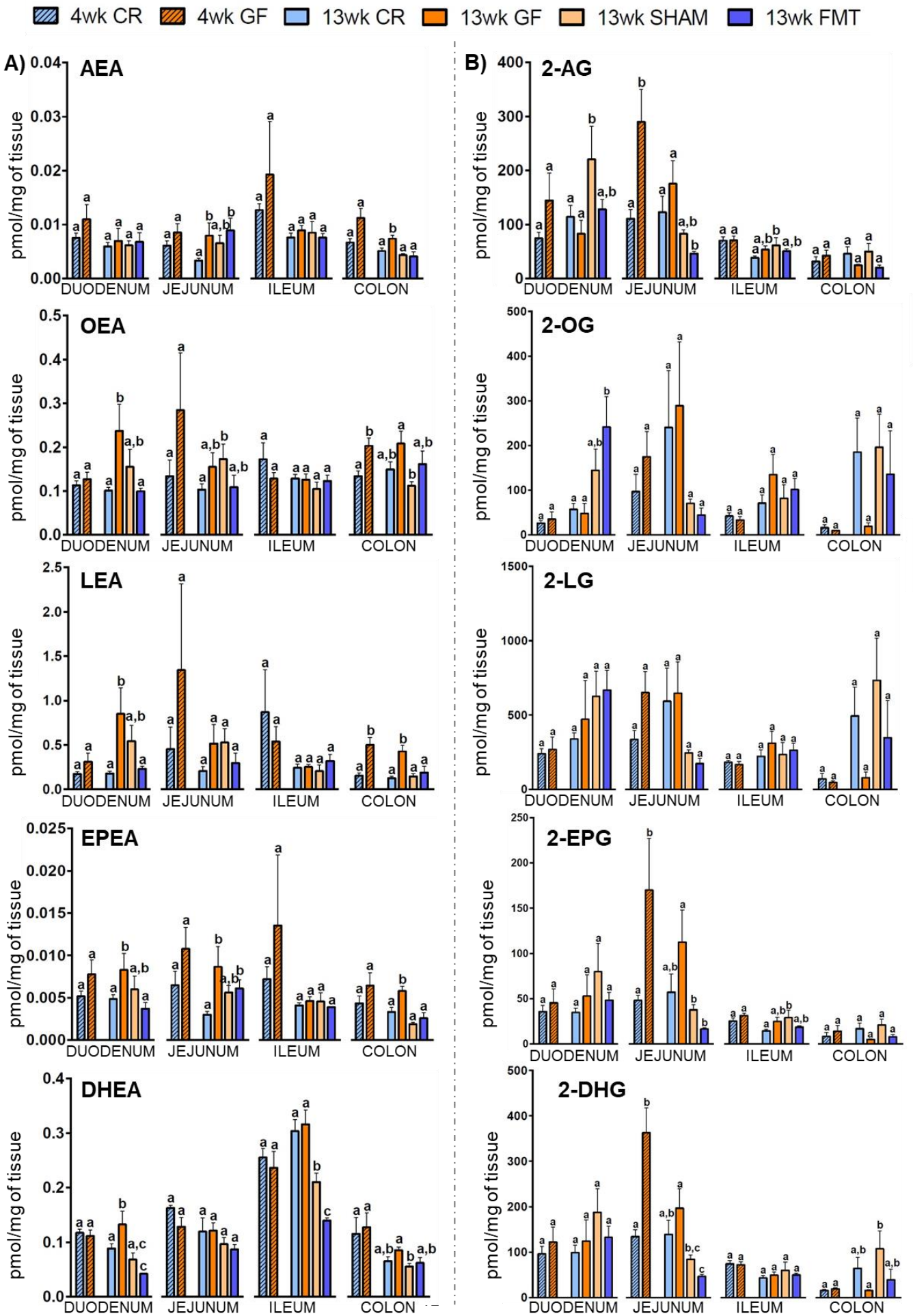

Fig. 3: Concentrations in intestinal tissues of endocannabinoids and select congeners in 4 and 13wk old conventionally raised (CR) or germ free (GF) mice and in 13wk old male GF mice gavaged with sterile PBS (SHAM) or fecal microbiota (FMT). Levels of *N*-acylethanolamines **(A)** and 2-acylglycerols **(B)** are expressed as pmol/mg of tissue and were determined in duodenum, jejunum, ileum and colon. Values are mean ± S.E.M of n=5-10. Bars marked with different letters were significantly different at the P≤0.05 level. AEA, anandamide; OEA, *N*-linoleoyl-ethanolamine; EPEA, *N*-eicosapentaenoyl-ethanolamine; DHEA, *N*-docosahexaenoyl-ethanolamine; 2-AG, the three enantiomers of mono-arachidonoyl-glycerol (added together because presumably coming from the isomerization of 2-arachidonoyl-glycerol); 2-OG, 2-oleoyl-glycerol; 2-LG, 2-linoleoyl-glycerol; 2-EPG, the three enantiomers of mono-eicosapentaenoyl-glycerol (added together because presumably coming from the isomerization of 2- eicosapentaenoyl -glycerol); 2-DHG, the three enantiomers of mono-docosahexaenoyl-glycerol-glycerol (added together because presumably coming from the isomerization of 2- docosahexaenoyl -glycerol).

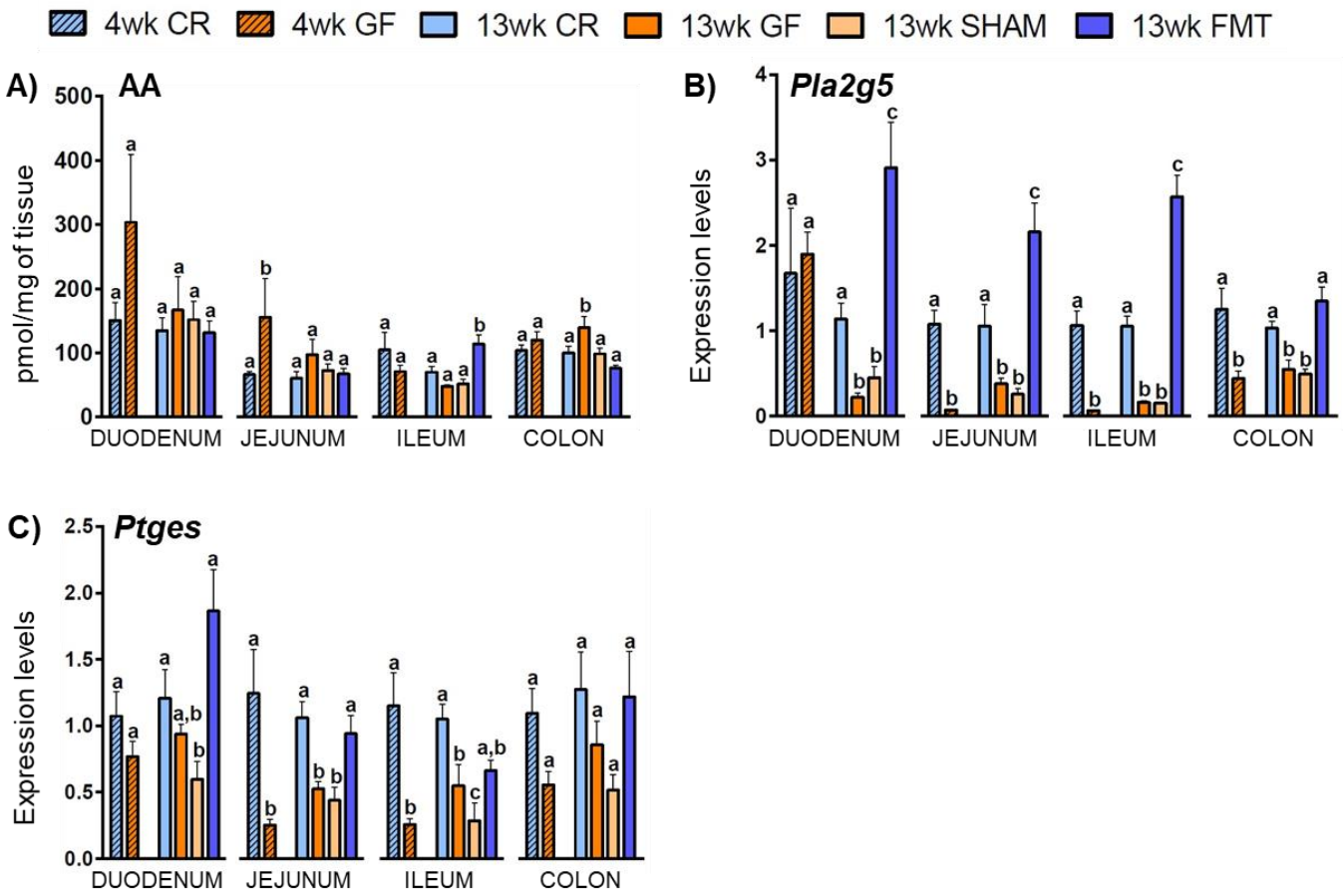

Fig. 4: Concentrations of arachidonic acid (AA) expressed as pmol/mg of tissue **(A)** and mRNA expression levels of *Pla2g5* **(B)** and *Ptges* **(C)** in 4 and 13wk old male conventionally raised (CR) or germ free (GF) mice and in 13wk old male GF mice gavaged with sterile PBS (SHAM) or fecal microbiota (FMT). Values are mean ± S.E.M of n=5-10. Bars marked with different letters were significantly different at the $p \leq 0.05$ level.

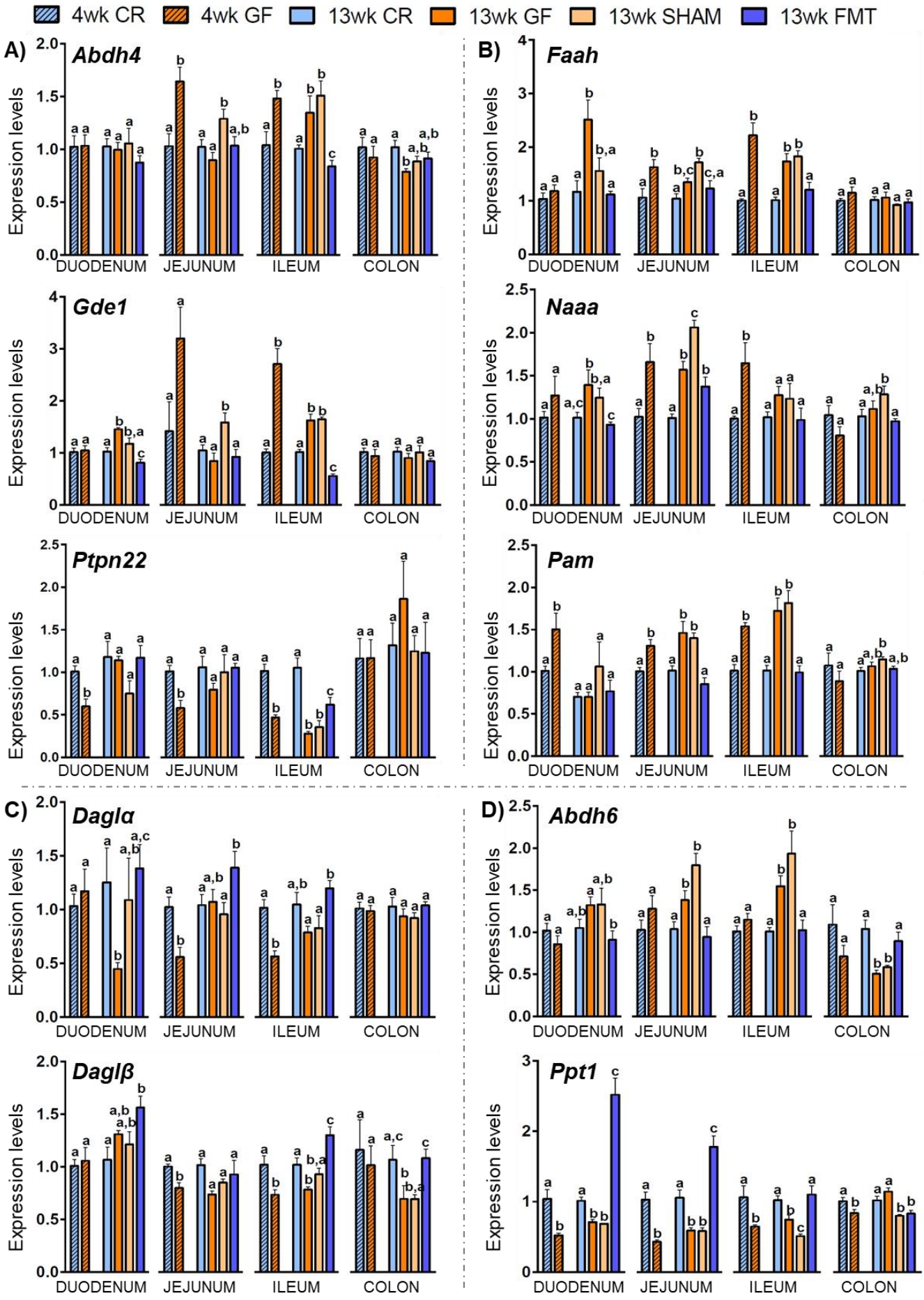

Fig. 5: Expression levels of select intestinal eCBome related anabolic and catabolic enzymes for *N*-aminoacylethanolamines **(A** and **B** respectively**)** and 2-acylglycerols **(C** and **D** respectively**)** in 4 and 13wk old male conventionally raised (CR) and germ free (GF) mice and in 13wk male GF mice gavaged with sterile PBS (SHAM) or fecal microbiota (FMT). The mRNA expression levels of all the genes represented were measured by qPCR array in duodenum, jejunum, ileum and colon for all experimental groups. Values are mean ± S.E.M. of n=5-10. Bars marked with different letters were significantly different at the $p \leq 0.05$ level.

JOURNAL OF LIPID RESEARCH

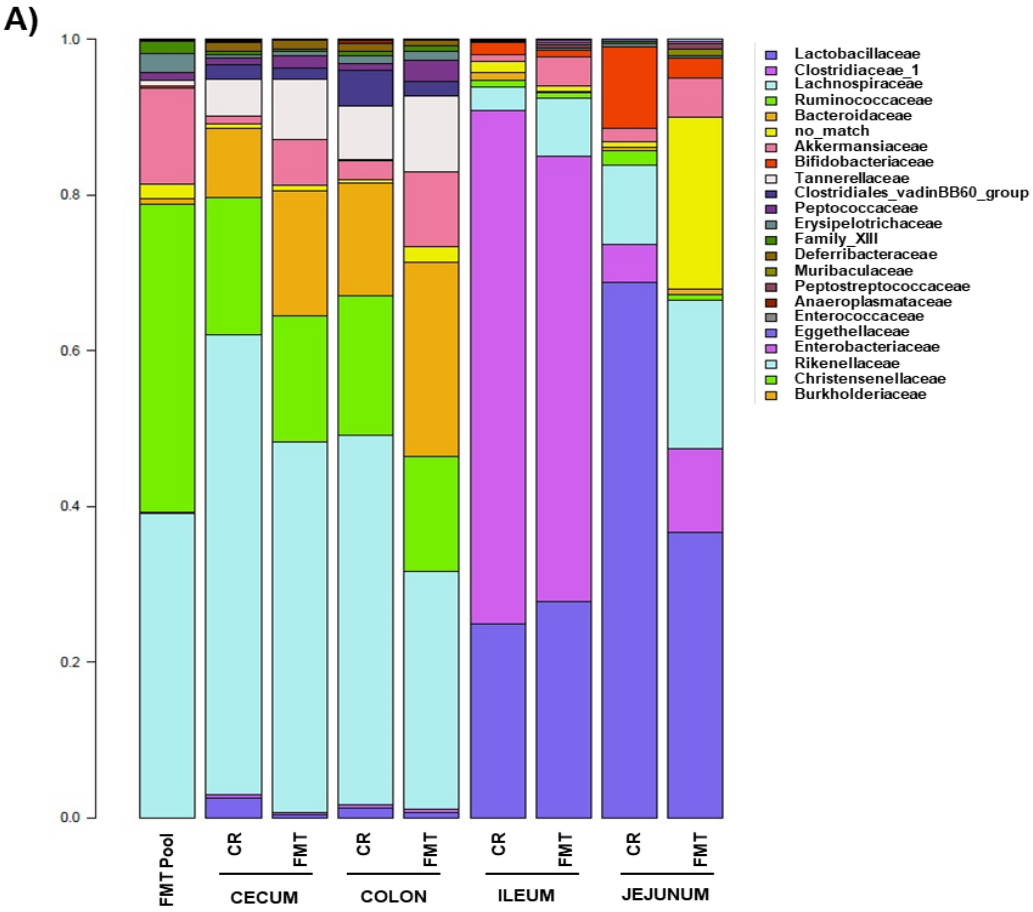

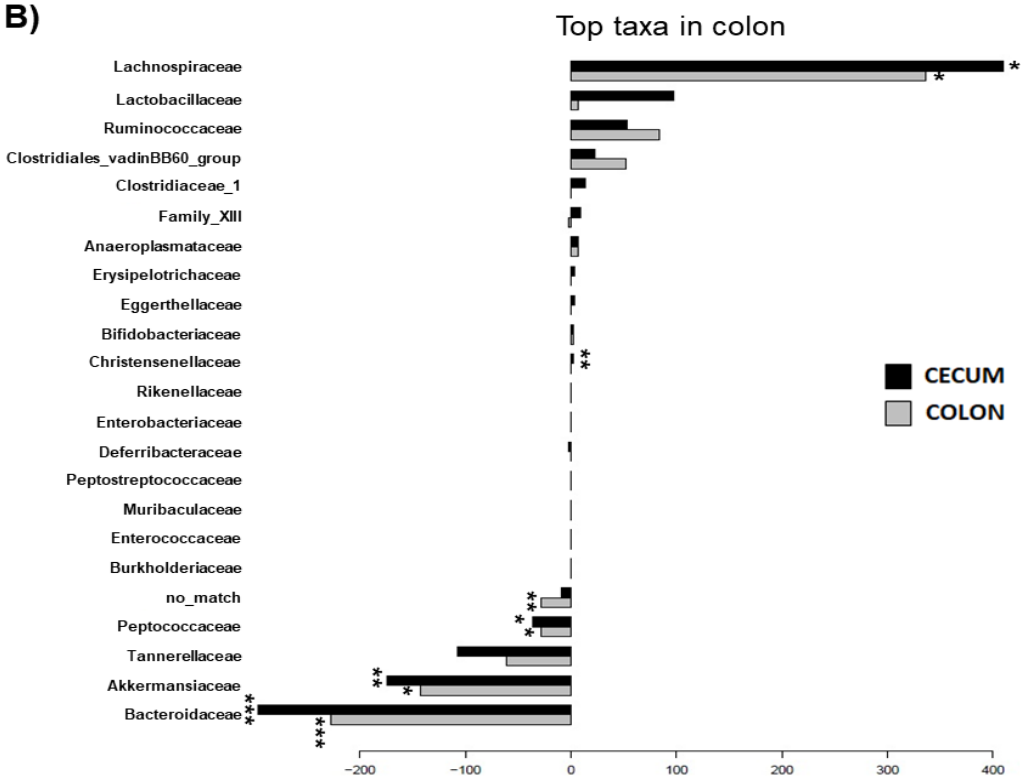

Fig. 6: Composition of the intestinal microbiome of 13wk old male germ-free mice after fecal microbiota transfer (FMT) and in conventionally raised (CR) mice. **A)** Average bacterial family composition of different intestinal segments (jejunum, ileum, colon and cecum) in CR and FMT mice, and in the intestinal contents and faeces pool (FMT pool) used for microbiota transfer. Family names (right) are presented from most (top) to lease (bottom) abundant. **B)** Comparison of colon and cecum microbiota composition of FMT mice and CR mice. Barplots show the coefficient associated bacterial families after permanova analysis. Positive values indicate a higher prevalence in CR mice and negative indicate a higher prevalence in FMT mice. * p≤0,05; ** p≤0,01; *** p≤0,005.